Arabian Journal for Science and Engineering
https://doi.org/10.1007/s13369-026-11230-0

RESEARCH ARTICLE-CIVIL ENGINEERING

Static and Dynamic Behavior of Elastic Circular Non-Local Plate Dynamics on Unilateral Two-Parameter Foundation by Using Chebyshev Polynomial Expansion

Zekai Celep[1] · **Cenk Aksoylar**[1] · **Hasim Cayir**[1]

Received: 19 November 2025 / Accepted: 2 March 2026

Abstract

This paper investigates the static and dynamic response of an elastic circular plate, focusing on forced vibrations. The plate is modeled as resting on a unilateral two-parameter foundation and subjected to both rotationally symmetric distributed and concentrically applied concentrated loads, all of which are time-dependent. The two-parameter foundation model incorporates non-local properties, and the plate is assumed to exhibit non-local elastic behavior. Additionally, the foundation is considered unilateral, accounting for potential separation between the foundation and the plate. The present study incorporates two characteristic parameters of the nonlocal foundation g_o and the plate μ to capture size effects of the foundation and plate. Within this framework of these assumptions, the static and dynamic behavior of the plate is studied by deriving the lift-off condition of the plate from the foundation. The governing equation of the system is formulated by accounting for the foundation beyond the contact region. An approximate solution is obtained using the Galerkin method. Given the rotational symmetry of the plate geometry and loading, the displacement function is assumed to have the same symmetry and is expressed using a symmetric Chebyshev polynomial expansion, which includes the contact region. To address a broad range of foundation, plate and load parameters, special attention is given to adopting non-dimensional parameters. Because of the nonlinear response of the unilateral foundation, numerical treatment is performed using an iterative solution procedure in the static case. Detailed numerical solutions are presented to investigate both static and dynamic behaviors of the plate. For dynamic loads, the second-order differential equation of motion is solved numerically using constant acceleration procedures. The effects of the plate and the foundation parameters are studied under various loading scenarios for both static and dynamic cases. Although arbitrary time variations are assumed for the loading, a stepwise time increment is employed in the numerical analysis for both concentrated and uniformly distributed loads, with forced vibration studied comparatively. Numerical results are presented to offer insight into the time variations of the contact region and the displacements at both the center and edge of the plate, for various plate and foundation parameters. Plate lift-off which induces nonlinear behavior is evidenced by the results presented. The effect of unilateral foundation characteristics on the static and dynamic behavior of the circular plate is illustrated through a comprehensive parameter analysis.

Keywords Elastic circular plate · Unilateral support · Static and dynamic response · Forced vibrations non-local foundation · Non-local plate

1 Introduction

The application of plates on elastic foundations is prevalent across a range of engineering fields, encompassing the structural, geotechnical, mechanical, and aerospace disciplines. This broad applicability has sustained ongoing interest in understanding the static and dynamic behaviors of plates on elastic foundations [1]. Among the various plate shapes, circular and rectangular plates are the most commonly used, with applications in engineering structures, for instance,

✉ Zekai Celep
zcelep@fsm.edu.tr

[1] Department of Civil Engineering, Faculty of Engineering, Fatih Sultan Mehmet Vakıf University, TR-34015 Zeytinburnu, Istanbul, Türkiye

Published online: 03 April 2026

machine parts, building slabs, and aircraft wings. Extensive investigations on design and verification analyses can be found in engineering literature, based on approximate, numerical, analytical, and semi-analytical techniques.

In these analyses, various foundation models of increasing complexity have been proposed to represent the soil, which inherently exhibits sophisticated behavior. One of the simplest models is the Winkler model. In the Winkler foundation model, the foundation reactions are assumed to be a linear function of the displacements. Furthermore, it is assumed that the foundation responds to both compression and tension in the same manner and remains in continuous contact with the structure, simplifying the analysis considerably. This conventional model treats the soil as consisting of separate elastic springs. However, this assumption becomes questionable when the transmission of tensile reactions between the structure and the soil is considered. The challenge in problems involving only compressive support is the consideration of separation between the structure and the foundation. The separation and contact regions are not known as a priori and depend on the parameters of the foundation, structure, and loading. The onset of support separation introduces nonlinearity into the analysis, typically requiring iterative numerical techniques. Due to this difficulty, studies involving unilateral, i.e., tensionless, Winkler foundations, are relatively limited. The inclusion of time-dependent loads further restricts these studies, as incorporating inertia forces complicates the solution. Research involving circular and rectangular plates on unilateral Winkler foundations is more common, particularly when considering circular and Cartesian symmetry. Often, iterative numerical techniques are employed to solve the problem's governing nonlinear equations.

Analyses of structures supported by several foundation types have been examined by Kerr [2–4], where it is pointed out that for a beam supported by a Winkler base, the load level affects the separation point location between the beam and the foundation. He pointed out that an intuitive approach to defining boundary conditions can yield erroneous assumptions.

The static response of plates supported by unilateral Winkler foundations has been the subject of extensive research. Weitsman [5, 6] examined an infinitely extended plate on an elastic foundation that reacts only in compression, under the action of a concentrated load. Special consideration was devoted to the mechanism by which the plate separates from the foundation. Kamiya [7] analyzed the axisymmetric response of a circular plate, clamped at its outer edge, resting on a bi-modulus unilateral foundation. The extent of the lift-off region in unilateral foundation has often been of particular interest, especially when the perimeter of the plate is completely free or simply supported, allowing for potential separation from the support. Villaggio [8] investigated a rectangular plate supported on a unilateral Winkler foundation, assuming the plate to be weightless and subjected to a concentrated load at its midpoint. The study focused particularly on the configuration of the contact region where the foundation separates from the plate. Dempsey et al. [9–12] studied the detachment of the edges of a simply supported rectangular plate on a unilateral foundation, assuming the supports could only transmit compression. They assessed the boundaries of the lift-off region and evaluated the compressive support reactions to check vertical equilibrium.

Numerous investigations have addressed the behavior of plates under unilateral support from elastic foundations. Ascione and Grimaldi [13] studied the static response of an elastic plate with the foundation modeled as a half-space, incorporating the possibility of lift-off. Kocatürk [14], Akbarov and Kocatürk [15] explored the effect of the plate's orthotropy. Hong, Teng, and Luo [16] studied axially symmetric plates and shells on an elastic tension-free foundation using the finite element method. A method for the numerical analysis of plates on unilateral elastic foundations was developed by Silva, Silveira, and Goncalves [17], in which the finite element method was employed for the discretization of both the foundation and the plate. Some of the static problems were generalized to include dynamic loads, resulting in forced vibration oscillations of the plate. A comprehensive review of plates and beams on elastic foundations, including numerical methods, was provided by Wang, Tham, and Cheung [18]. Considering practical significance, the dynamic behavior of rigid footings supported by tension-free elastic Winkler foundations is examined by Psycharis [19]. Al-Shugaa, Musa, and Al-Gahtani [20] employed energy and Ritz techniques to analyze thin plate bending behavior on non-homogeneous foundations. The accuracy of the obtained solution was enhanced through the incorporation of the fundamental solution into the polynomial expression. This approach effectively enhanced the precision of natural boundary conditions along the plate's free edges and enabled the accurate representation of singularities occurring at the internal column supports.

A circular plate on a unilateral Winkler support, loaded uniformly over a circular arc, is analyzed by dividing it into two cylindrical regions. Continuity at the interface and unilateral simply supported edge conditions are imposed (Celep, Turhan, and Al-Zaid [21]). Celep [22] investigated a free circular plate resting on a unilateral Winkler base under an eccentric vertical load, minimizing the total potential energy of the system. In their study, Celep, Turhan, and Al-Zaid [23] analyzed the contact interaction between a unilateral Winkler foundation and a circular plate by utilizing the free vibration mode shapes of a fully free plate, with the lift-off boundary condition approximated through a harmonic averaging technique.

Celep and Turhan [24] investigated the axisymmetric vibrations of a circular plate subjected to a time-dependent concentrated vertical dynamic load, assuming the plate rests on a unilateral foundation. The solution was obtained using the Galerkin method and the modal functions of the completely free plate. Celep [25] studied the responses of a plate-column system on a unilateral Winkler foundation, subjected to free vibration, harmonic ground motion, and the El Centro 1940 earthquake. Güler and Celep [26] presented the static and dynamic behavior of a circular plate on a unilateral Winkler support, using the Galerkin approach and assuming the plate is subjected to vertical loads and centric external moments which are time-dependent. Celep et al. [27, 28] investigated a rigid circular plate supported by a unilateral Winkler foundation along its edge under static and dynamic loads, as well as the behavior of a circular elastic plate on a tensionless foundation. In the latter work, the geometry and the load were assumed to be rotationally symmetric, and the analysis was conducted using the Galerkin method.

The Pasternak and Wieghardt foundation models, which are two-parameter models, can be considered a non-local extension of the Winkler model. In this model, the displacement at a point on the foundation depends not only on the external pressure at that point but also on the external pressure at neighboring points. Celep, Güler, and Demir [29–32], Dimitrovova [33], and Ghafarian and Ariaei [34] have conducted studies on the static and dynamic response of beams, plates, and rectangular plate-column systems resting on tensionless Pasternak foundations. Various solution techniques, including the minimum potential energy method, the Galerkin method, and the use of Lagrange equations, are available in the literature presented by Celep et al. [35–40], Dang et al. [41]. The use of Chebyshev polynomials for the displacement series of plates has found several applications in solving problems for plates of triangular and rectangular shapes, taking advantage of their completeness and rapid convergence properties, as well as their definition on a finite interval as given by Celep et al. [42–45] and Huang et al. [46]. One of these studies investigates a rectangular plate supported by a two-parameter unilateral foundation under static and dynamic loads, similar to the analysis presented for the circular plate in this study. In the study, there are governing equations of the nonlocal Mindlin plate theory for bending of magnetoelectroelastic nanoplates resting on the Pasternak elastic foundation using the variational principle by Feng et al. [47]. For the governing equations of the bending problem, the method of the polynomial particular solutions is developed. The new method enables to consider the effects of different boundary conditions, applied loads, and geometrical shapes on the bending properties of the nanoplates. It is shown that the presence of nonlocal effect can increase the absolute values of the deflection and rotation. A nonlinear static analysis of a circular/annular nanoplate on the Winkler–Pasternak elastic foundation based on the nonlocal strain gradient theory is presented by Sadeghian et al. [48], considering circular geometry. Solution of the governing equations in circular coordinates is accomplished by applying the differential quadratic method. The results show that displacement of the plate decreases with the increasing order of the shear deformation theory and the increase in the strain gradient parameter and causes decreases in the non-dimensional maximum deflection of the nanoplate. A non-classical model for a Mindlin plate on a two-parameter Winkler–Pasternak foundation model foundation is developed using a modified couple stress theory including a surface elasticity theory by Gao and Zhang [49], and the solutions of the static bending and free vibration of a simply supported rectangular plate are presented an illustrative example for the new plate model. Foyouzat and Mofid [50] presented solution for the static bending response of an axisymmetric thin circular/annular plate with different boundary conditions on Winkler foundation by adopting infinite power series expansion of the deflection function employed. The method is applied to plates having free, clamped, hinged, and elastically restrained boundaries.

Nonlocal elasticity theory in mechanical modeling of the structures assumes that the state of stress at a given point in a material is determined not only by the state of strain at that point, but also by the state of strain of the neighboring points accepting that its effect decreases with distance at other points. In the two-parameter soil model considered here, the displacement at any point is assumed to be affected by the foundation reaction of all points of the soil in a way that decreases with distance. From this perspective, this two-parameter foundation model also has a nonlocal characteristic. In this study, an attempt is made to study the behavior of the plate by combining the nonlocal characteristics of the plate and the soil, and the dependence of the results on the nonlocal parameters is examined.

Unlike the aforementioned studies which generally consider bilateral (bonded) contact, in the present study, a completely free circular plate supported by a unilateral (tensionless) two-parameter elastic foundation is considered. Foundation is modeled as a combination of elastic springs, similar to the Winkler foundation and an elastic membrane that provides interactions between the springs. This interaction ensures that the two-parameter foundation exhibits non-local behavior. The circular plate is assumed to be subjected to a rotationally symmetric uniformly distributed load and a concentrically applied concentrated force. Since the geometry, boundary conditions, and the loading of the problem exhibit rotational symmetry, this property is incorporated into the derivation of the governing equation and the solution process. The governing equation is achieved by combining the equations of the linear elastic non-local

plate with the two-parameter unilateral foundation model. In this approach, both the foundation and the plate can be considered as a generalization of the Winkler foundation and Kirchhoff plate, respectively, by incorporating non-local properties into both. Furthermore, since it is well known that no tensile reaction can be transmitted between the foundation and the plate, the foundation is assumed to be unilateral. Owing to this unilateral property, separation between the foundation and the plate is taken into account, resulting in a governing equation with pronounced inherent nonlinearity. Separation condition is developed in the two-parameter foundation and implemented in the numerical solution. In solution, the displacement field is expressed as a series of Chebyshev polynomials in the radial direction, ensuring that rotational symmetry is satisfied. The static and dynamic behavior of the plate is investigated, with numerical findings presented in comparative figures. To validate and assess the accuracy of the proposed formulation, particular attention is given to the displacements of the plate, the extent of the contact region, and the equilibrium of the vertical forces. Global vertical equilibrium of the forces applied to the plate is developed and numerically checked in the static solution and in every time step of the dynamic solution which can be considered as a numerical inspection of the numerical solution. This check serves as a validation of the numerical stability and acts as a residual check for the dynamic solution, ensuring that the equations of motion are satisfied at each time step. The analyses are carried out for both static and dynamic cases in which inertial effects are also taken into account. Certain results are compared with those obtained using the SAP2000 software [51].

In this study, since the two-parameter foundation is considered, an additional edge force comes into being due to the second foundation parameter at the outer edge of the completely free plate, the vertical component of which affects the plate shear force, when the plate is completely contact with the foundation. The reason this term is not seen in the most solutions is that the plate is often considered to be simply or built-in supported at its relevant edge, and this term appears as a part of the support reaction and does not affect the edge boundary condition. The condition regarding the separation of the plate from the foundation in the two-parameter foundation is also given depending on the properties of the foundation parameters. Care has been taken to write the governing equation with the selected dimensionless parameters, to obtain the numerical solutions using these dimensionless parameters, and to interpret the results accordingly.

2 Non-Local Foundation Model

Since the problem is rotationally symmetric, the governing equations for the foundation model are provided for this specific case for brevity. The Winkler foundation assumes that the foundation consists of unconnected elastic springs, with the deflection of the foundation $W(R)$ is directly proportional to the foundation reaction $P_f(R)$ at the same point,

$$W(R) = P_f(R)/K_o \tag{1}$$

which is a linear local elastic foundation model that establishes a one-to-one relationship between displacement and foundation reaction at the point of interest. The proportionality coefficient K_o is referred to as the foundation spring stiffness. This model is generalized by Pasternak and Wieghardt by incorporating a second parameter, as given by Capurso [52], in polar coordinates for the rotationally symmetric case

$$W(R) = \frac{1}{G_o}\int_{-\infty}^{+\infty}\int_{-\infty}^{+\infty} \overline{K}_o(\beta\lambda) P_f(\overline{R})\overline{R}d\overline{R} \tag{2}$$

where $\overline{K}_o(\beta\lambda)$ is the modified Bessel function of the second kind of zero order, and $\lambda = \left|R - \overline{R}\right|$ is the distance between the point (R) where the displacement is evaluated and the point $(\overline{R})$ where the kernel function represents interaction between the two points and $\beta^2 = G_o/K_o$. The displacement at a point on the foundation depends not only on the external pressure at that point but also on the external pressure at neighboring points. This model can, therefore, be considered a non-local elastic foundation model. The corresponding mechanical model generalizes the Winkler model by adding a shear layer or a stretched membrane on the Winkler springs, where G_o corresponds to the tensile force of the stretched membrane and denotes a membrane stiffness of the foundation. The integral relationship (2) can be expressed in an equivalent differential form in cases exhibiting rotational symmetry:

$$P_f(R, t) = K_o W(R, t) - G_o\left(\frac{\partial^2 W}{\partial R^2} + \frac{1}{R}\frac{\partial W}{\partial R}\right) \tag{3}$$

3 Non-Local Plate Model

Since the rotationally symmetric problem is considered, the governing equations of the model of the foundation and plate are given for this case only. According to the classical elasticity developed for a Hookean solid, the strain $\boldsymbol{\varepsilon}(R)$ is related to the stress $\boldsymbol{\sigma}(R)$ at the same point, i.e., $\boldsymbol{\sigma} = \mathbf{C}\boldsymbol{\varepsilon}$, where $\mathbf{C}$ is the elasticity tensor. In the non-local elasticity, it is assumed that stress at a point is a function of the strains at all points in the structural element, with the influence decreasing inversely with the distance from the specific point. The Hooke's law

for the stress–strain relationship in the non-local elasticity, as described by Eringen [53], can be expressed in a rotationally symmetric case as follows,

$$\boldsymbol{\sigma}(R) = \int_0^{+\infty} K(\lambda)\mathbf{C}''(\overline{R})d\overline{R} \tag{4}$$

where $K(\lambda) = K(|R - \overline{R}|)$ denotes the kernel function which establishes the non-local interaction between points and reaches to its maximum at $R = \overline{R}$ and attenuates for large distance, displays analogous to a Dirac delta function, and includes an internal characteristic length for the material. This stress–strain relationship can be expressed as follows as well,

$$(1 - \mu^2\Delta)\boldsymbol{\sigma} = \mathbf{C}\boldsymbol{\varepsilon} \tag{5}$$

where $\mu^2 = e_o^2 a^2$ is the non-local parameter, which includes the characteristic length, $\boldsymbol{\sigma}$ is the stress tensor and $\boldsymbol{\varepsilon}$ is the strain tensor and $\mathbf{C}$ is the elasticity tensor which includes the material parameters. The nonlocal theory of elasticity proposed by Eringen [53] has been widely used in many nanomechanical problems including wave propagation, vibration analysis of nanobeams, nanotubes, carbon nanotubes, and microtubes. The theory includes scale effects to include tthe nonlocal effects in the materials. The characteristic length represents the non-local interaction between the neighboring points. When the characteristic length approaches zero, i.e., $\mu \to 0$ non-local elasticity reduces to the conventional local elasticity. For a two-dimensionally rotationally symmetric case the equation

$$\left[1 - \mu^2\left(\frac{d^2}{dR^2} + \frac{1}{R}\frac{d}{dR}\right)\right]\begin{bmatrix}\sigma_{rr}\\ \sigma_{\theta\theta}\end{bmatrix} = \frac{E}{1-\nu^2}\begin{bmatrix}1 & \nu\\ \nu & 1\end{bmatrix}\begin{bmatrix}\varepsilon_{rr}\\ \varepsilon_{\theta\theta}\end{bmatrix} \tag{6}$$

By using these constitutive equations, the equations for bending moment and shearing force of the non-local circular plate for having rotationally geometry and loading can be driven as follows,

$$\left[1 - \mu^2\left(\frac{d^2}{dR^2} + \frac{1}{R}\frac{d}{dR}\right)\right]\begin{bmatrix}M_{rr}\\ M_{\theta\theta}\end{bmatrix} = -D\begin{bmatrix}1 & \nu\\ \nu & 1\end{bmatrix}\begin{bmatrix}\frac{d^2W}{dR^2}\\ \frac{1}{R}\frac{dW}{dR}\end{bmatrix} \tag{7}$$

$$\left[1 - \mu^2\left(\frac{d^2}{dR^2} + \frac{1}{R}\frac{d}{dR}\right)\right]V_{rr} = -D\frac{d}{dR}\left(\frac{d^2W}{dR^2} + \frac{1}{R}\frac{dW}{dR}\right) \tag{8}$$

The Cartesian form of these equations is found in the study by Nami and Janghorban [54] and Papargyri-Beskou and Beskos [55]. By using the equations above the governing equation of the plate having circular symmetry can be obtained as follows,

$$\begin{aligned} &D\left(\frac{\partial^2}{\partial R^2} + \frac{1}{R}\frac{\partial}{\partial R}\right)\left(\frac{\partial^2 W}{\partial R^2} + \frac{1}{R}\frac{\partial W}{\partial R}\right)\\ &= \left[1 - \mu^2\left(\frac{\partial^2}{\partial R^2} + \frac{1}{R}\frac{\partial}{\partial R}\right)\right]\\ &\quad\times\left[Q(R,t) - m\frac{\partial^2 W}{\partial t^2} - P_f(R,t)\right] \end{aligned} \tag{9}$$

where m is the mass per unit area, h is the thickness of the elastic circular plates, E and G are the moduli of elasticity and shear, ν is Poisson's ratio, and $D = E h^3/12(1-\nu^2)$ bending stiffness of the plate. In the governing equation ordinary differentiations are written as partial differentiations to include the time variations of the loads $Q(R, t)$, the displacement function $W(R, t)$, and the foundation pressure $P_f(R, t)$. Correspondingly the governing equation includes the inertia forces.

4 Analysis of Circular Plate on Elastic Foundation

A circular elastic plate, shown in Fig. 1, is considered to be resting on a unilateral elastic two-parameter foundation characterized by a spring stiffness K_o, together with a surface membrane carrying a tensile force G_o, as illustrated in Fig. 1a. It is assumed that the plate is subjected to a rotationally distributed load $Q_o(R, t)$ and a concentrated load $P_o(t)$ acting at its center. Since these loads are a function of time, the plate displacements are also dependent on the time, $W(R, t)$. Because the unilateral foundation responds solely to compression, i.e., $P_f(R, t) \geq 0$, lift-off and contact regions having rotationally symmetry are expected. Reaction of the two-parameter foundation can be written as follows as given in Fig. 1d,

$$P_f(R,t) = H(R,t)\left[K_o W(R,t) - G_o\left(\frac{\partial^2 W}{\partial R^2} + \frac{1}{R}\frac{\partial W}{\partial R}\right)\right] \tag{10}$$

where unilateral property of the foundation is included by employing a contact function $H(R, t)$ taking the form of a Heaviside function, in order to represent tensionless foundation as follows (Fig. 1(b, c)):

$$H(R,t) = 1 \quad \text{for} \quad K_o W(R,t) - G_o\left(\frac{\partial^2 W}{\partial R^2} + \frac{1}{R}\frac{\partial W}{\partial R}\right) \geq 0 \qquad R \leq R_{\text{contact}}$$

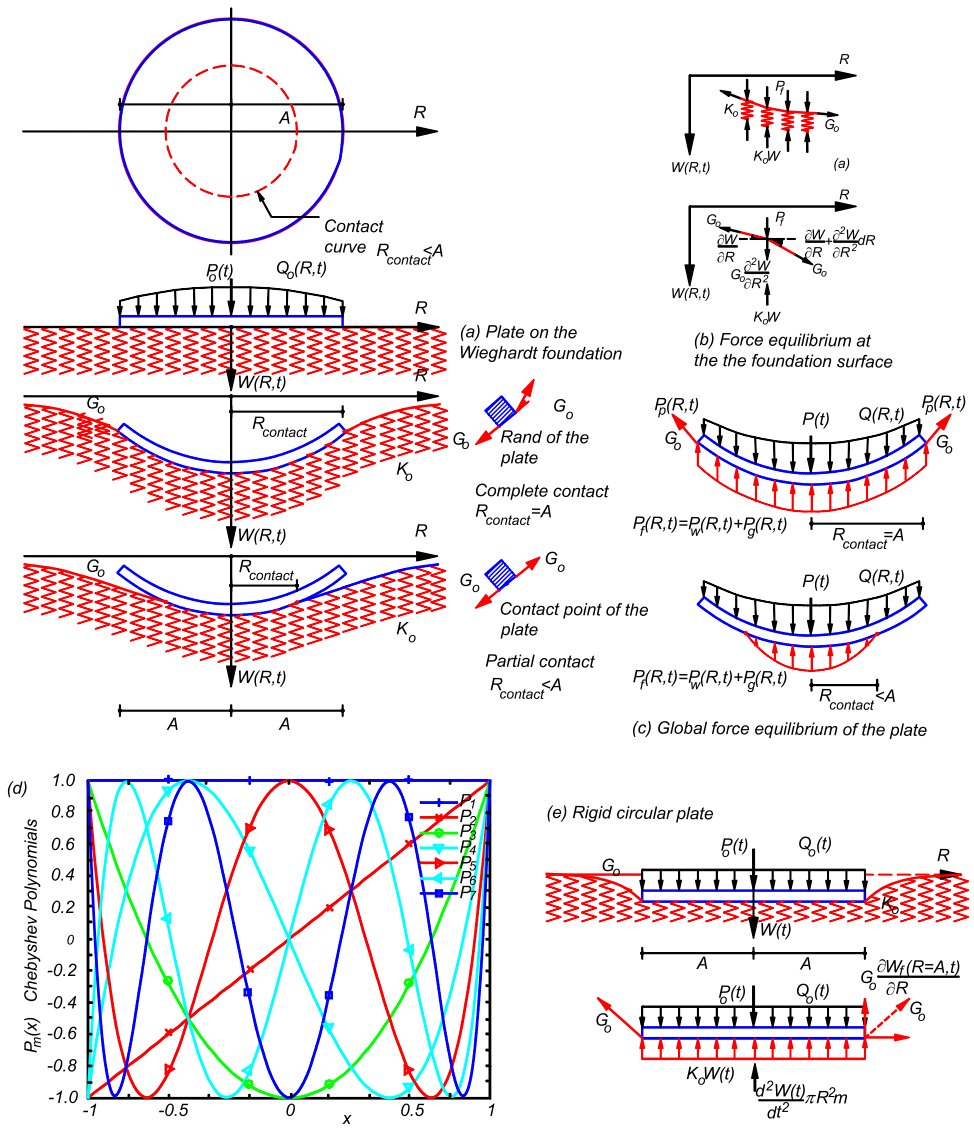

Fig. 1 **a** Geometry and coordinate system of a circular plate supported by Wieghardt (two-parameter) foundation and subjected to a rotationally symmetric distributed load $Q_o(t, R)$ and a concentrated force $P_o(t)$ at the center of the plate, **b** force equilibrium at the foundation surface, **c** global force equilibrium of the plate, **d** Chebyshev polynomials, and **e** rigid circular plate

$$H(R,t)=0 \quad \text{for} \quad K_oW(R,t)-G_o\left(\frac{\partial^2 W}{\partial R^2}+\frac{1}{R}\frac{\partial W}{\partial R}\right) \leq 0 \qquad R \geq R_{\text{contact}} \tag{11}$$

In the two equations above, the non-local character of the foundation is presented due to differential operators in the equations above. As it is seen in Fig. 1, the displacement function and its derivatives reach zero at the contact point where the effect of this Heaviside function begins, so the Heaviside function does not cause a sudden jump in the displacement function and its derivatives and their smooth variations continue. This smoothness condition prevents numerical chattering during the dynamic contact update. While the contact point is obtained iteratively in the static solution using the contact condition (11), in the dynamic solution, the contact point can be evaluated easily due to the smooth variation along the time direction. There is only a discontinuity in the derivative of the displacement function at the edge of the plate at the complete contact, which causes an edge force to appear due to the surface tensile force of the foundation G_o.

The characteristic length, as defined in the non-local elasticity, corresponds to $\sqrt{G_o/K_o}$ in the two-parameter foundation model. Therefore, the governing equation of the displacement function $W(R, t)$ can be derived by incorporating the effects of both the unilateral two-parameter foundation and the external forces, including the inertia force, under circular symmetry, as follows:

$$L_d(R,t)=D\left(\frac{\partial^2}{\partial R^2}+\frac{1}{R}\frac{\partial}{\partial R}\right)\left(\frac{\partial^2 W}{\partial R^2}+\frac{1}{R}\frac{\partial W}{\partial R}\right)+\left[1-\mu^2\left(\frac{\partial^2}{\partial R^2}+\frac{1}{R}\frac{\partial}{\partial R}\right)\right]$$

$$\times \left[H(R,\, t)\left[K_o W(R,\, t) - G_o\left(\frac{\partial^2 W}{\partial R^2} + \frac{1}{R}\frac{\partial W}{\partial R} \right) \right] + m\frac{\partial^2 W}{\partial t^2} - Q(R,\, t) - P_o(t)\delta(R=0) \right] = 0 \quad (12)$$

where the last two terms corresponding to the rotationally symmetric distributed load $Q(R,\, t)$ and external concentrated load $P_o(t)$ applied at the center of the plate and $\delta(R)$ denoting the Dirac Delta function. The last equation, which incorporates the non-local properties of both the foundation and the plate, represents a generalization of the plate governing equation as presented by Timoshenko and Woinowsky-Krieger [1]. In this case, obtaining an exact solution for the displacement function is highly challenging and may even be unattainable. Primarily due to the non-local properties of the plate and the foundation, as well as the unilateral nature of the foundation, which further complicates the analysis. Additionally, the time-dependent nature of dynamic problems and their initial conditions introduce another layer of complexity. Generally, the extent of the contact region on the unilateral support is influenced by both the parameters of the plate and the loading configuration. However, it is important to note that the assumed rotational symmetry simplifies the problem to some extent, ensuring that the lift-off and contact regions are circular in the case of the partial contact as well. Therefore, an approximate solution for the governing equation is sought here through the application of the Galerkin procedure.

For the application of the Galerkin procedure, the displacement function is assumed to be expressible in terms of Chebyshev polynomials of the first kind which satisfy the symmetry condition, i.e., exhibiting even variations [56].

$$W(R,\, t) = Aw(r,\, \tau) = A \sum_{m=1,\,3,\,5,\,\ldots}^{\infty} A_m(\tau) P_m(r) \quad (13)$$

where the first-type Chebyshev polynomials are defined as,

$$P_m(r) = \cos[(m-1)\text{arc}\, cos(r)] \quad m = 1,\, 3,\, 5,\, \ldots \quad (14)$$

The first seven Chebyshev polynomials are displayed in Fig. 1c. Governing equations of the elastic bodies and the essential and natural boundary conditions can be obtained by employing the principle of the work as discussed by Reddy [57]. Galerkin method is one of the weighted residual methods is developed by requiring that the coordinate functions which satisfy the essential boundary conditions are orthogonal to the residual function of the governing equation within the definition region of the problem. In the present analysis the application of the Galerkin method implemented not only the residue of the governing equation, to the residue of the boundary conditions as driven the principle of virtual work. As it is expected, when the admissible functions satisfy all the boundary conditions, this part will vanish. In this study, all boundary conditions are incorporated into the governing Eq. (12) before applying the Galerkin method. This approach enhances the accuracy of the numerical results by minimizing errors arising from the failure of satisfying non-essential boundary conditions. Specifically, the boundary conditions at the free edge of the circular plate are properly included in the governing equation to account for their effects and enhance the accuracy of the approximation. The application of the Galerkin method is then carried out as follows:

$$\int_0^A L_d[W(R,\, t)] P_n(R) R\, dR + L_b[R = A,\, t,\, P_n(R=A)] = 0 \quad n = 1,\, 3,\, 5,\, \ldots \quad (15)$$

where the second part includes the effects of the boundary conditions at the edge of the plate which are not satisfied, i.e., the shear force and the bending moment free conditions

$$\begin{aligned} L_b[R = A,\, t,\, P_n(R=A)] &= \left[P_n(R)\left[1 - \mu^2\left(\frac{\partial^2}{\partial R^2} + \frac{1}{R}\frac{\partial}{\partial R} \right) \right] V_{rr} \right]_{R=A} \\ &- \left[\frac{dP_n(R)}{dR}\left[1 - \mu^2\left(\frac{\partial^2}{\partial R^2} + \frac{1}{R}\frac{\partial}{\partial R} \right) \right] M_{rr} \right]_{R=A} \\ &+ G_o\left[\left(\frac{\partial W_f}{\partial R} \right)_{R=A^+} - \left(\frac{\partial W}{\partial R} \right)_{R=A^-} \right] \\ &\times H(R = A,\, t) P_n(R)_{R=A} = 0 \end{aligned} \quad (16)$$

Due to rotational symmetry of the problem the integration is carried along the radial direction and the second term is evaluated for $R = A$ only. In Eq. (16), the first term represents the shearing force, and the second term corresponds to the bending moment. The third term reflects the vertical component of the force resulting from the membrane stress of the second parameter in the two-parameter foundation model, as illustrated in Fig. 1. This term appears when the plate is in complete contact with the foundation, and the foundation surface has a discontinuity in slope at the edge of the plate. The last term is often overlooked in studies involving two-parameter foundations for various reasons. In fact, this term disappears when the edge of the plate lifts off. However, when a support is present at the edge of the plate, this term generates a vertical force that is directly transferred to the supports [45]. In Eq. (16), $W_f(R)$ represents the free surface of the foundation beyond the contact point and will be addressed later.

Before applying the Galerkin method to Eq. (15) and consequently to Eq. (16), the shear force V_{rr} and the bending moment M_{rr} given from Eqs. (6) and (7) have to be

expressed using the selected displacement functions (13) and substituted. The first and third terms together represent the boundary condition related to the shear force at the outer edge of the plate, and the second term represents the boundary condition related to bending moment. If the selected displacement functions satisfy the shear force boundary condition at the outer edge, the sum of the first and third terms will disappear; similarly, if they satisfy the bending moment boundary condition, the second term will disappear, and the application of the Galerkin method will not yield a remainder term.

Before applying the Galerkin method, a set of non-dimensional parameters is introduced for simplicity and clarity. This ensures that the subsequent conclusions and the numerical results remain valid across a wide range of parameter values.

$$p_o(\tau)=\frac{P_o(t)A}{D}\quad q_o(\tau)=\frac{Q_o(t)A^3}{D}\quad k_o=\frac{K_oA^4}{D}\quad g_o=\frac{G_oA^2}{D}$$
$$r=\frac{R}{A}\quad r_{\text{contact}}=\frac{R_{\text{contact}}}{A}\quad \tau=\frac{t}{T_p}\quad T_p^2=\frac{mA^4}{D}\quad \mu_o=\frac{\mu}{A} \tag{17}$$

where $Q_o(t)$ is considered as an uniformly distributed load. Use of the non-dimensional parameters ensures that the subsequent conclusions and the numerical results remain valid for a wide range of the parameter value, i.e., in this way, a very wide numerical range of the parameters of the problem is considered. In the graphical presentation of the numerical results, the numerical range of the parameters is chosen so that the effect of the nonlocal parameters can be seen. The use of dimensionless parameters also provides dimensional control in obtaining the governing equations of the problem. For instance, in the context of nanomechanics, the non-dimensional non-local parameter values (μ_o) explored here correspond to typical material length scales observed in graphene sheets or carbon nanotubes, whereas for macro-scale civil engineering structures, this parameter would naturally approach zero.

As is well known the Chebyshev polynomials are defined within the interval of $-1 \le r \le +1$ and include odd and even functions. Due to the symmetry in the present case only the even polynomials will be used for $0 \le r \le +1$ as shown in Fig. 1c. The first even Chebyshev polynomial $P_1(r) = 1$ represents the rigid translational displacement of the plate along the $w(r, \tau)$ axis. The higher-order even polynomials, such as, $P_3(r) = 2r^2 - 1$, $P_5(r) = 8r^4 - 8r^2 + 1$, …, represent plate displacements which result in elastic deformations. Since Chebyshev polynomials are mathematically complete orthogonal function sets, they are preferred as admissible coordinate functions. They offer several advantages as well, including relatively fast convergence and improved stability during numerical computations. These polynomials can provide acceptable approximations even by using fewer terms in the expansion and enable the extraction of effective solutions. Additionally, Chebyshev polynomials offer straightforward and uniform representation similar to the cosine expressions, which significantly enhances the efficiency of the analysis. However, in the present application, due to the rotational symmetry of the problem, only even polynomials within the interval $0 \le r \le +1$ are adopted, differing from the general use. The numerical treatment of the integrals involving Chebyshev polynomials is implemented using MATLAB [58]. Another strategy for choosing the displacement functions would involve using the rotationally symmetric free vibration mode functions of a completely free plate, which satisfy the boundary conditions completely. Nonetheless, this selection presents a numerical limitation, particularly due to the dealing of large numbers associated with the regular and modified Bessel functions of the first kind when higher vibration modes are considered.

The use of higher-order Chebyshev polynomials is intended to describe both rigid translation and elastic deformations. As expected, when the relative foundation stiffnesses k_o and g_o, with respect to the plate bending stiffness D, are relatively low, the contribution of rigid translation to the displacement of the plate becomes significant relative to elastic deformations. In this case, numerical accuracy can be achieved by considering only a minimal number of coordinate functions, such as Chebyshev polynomials, in addition to rigid translation. However, when the relative stiffnesses are large, the significance of the elastic deformations of the plate becomes more pronounced. In such cases, the numerical treatment requires relatively great number of coordinate functions, i.e., higher-order Chebyshev polynomials, to capture accurately the elastic deformations of the plate.

By utilizing non-dimensional parameters, the application of the Galerkin approach to the governing equation leads to the following:

$$\int_0^1 \overline{L}_d[w(r,\tau)]P_n(r)r\,dr + \overline{L}_b[r=1,\tau,P_n(r=1)]=0 \quad n=1,3,5,\ldots \tag{18}$$

where

$$\overline{L}_d(r,\tau)=\left(\frac{\partial^4 w}{\partial r^4}+\frac{2}{r}\frac{\partial^3 w}{\partial r^3}-\frac{1}{r^2}\frac{\partial^2 w}{\partial r^2}+\frac{1}{r^3}\frac{\partial w}{\partial r}\right)+\left[1-\mu_o^2\left(\frac{\partial^2}{\partial r^2}+\frac{1}{r}\frac{\partial}{\partial r}\right)\right]\times\left[H(r,\tau)\left[k_o w(r,\tau)-g_o\left(\frac{\partial^2 w}{\partial r^2}+\frac{1}{r}\frac{\partial w}{\partial r}\right)\right]+\frac{\partial^2 w}{\partial \tau^2}-q_o(\tau)-p_o(\tau)\delta(r=0)\right]$$

$\overline{L}_b[r=1,\tau,P_n(r=1)]$

$$= -\left[\left(\frac{\partial^3 w}{\partial r^3} + \frac{1}{r}\frac{\partial^2 w}{\partial r^2} - \frac{1}{r^2}\frac{\partial w}{\partial r}\right)P_n(r)\right]_{r=1} + \left[\left(\frac{\partial^2 w}{\partial r^2} + \frac{\nu}{r}\frac{\partial w}{\partial r}\right)\frac{dP_n(r)}{dr}\right]_{r=1} + g_o\left[\left(\frac{\partial w_f}{\partial r}\right)_{r=1^+} - \left(\frac{\partial w}{\partial r}\right)_{r=1^-}\right]H(r=1,\tau)P_n(r=1) \quad (19)$$

The insertion of the displacement function (13) into the functionals within the governing Eq. (18) yields to the expressions shown below:

$$\int_0^1 \sum_{m=1}^{\infty}[A_m P_m^{iv}(r) + \frac{2}{r}A_m P_m^{'''}(r) - \frac{1}{r^2}A_m P_m^{''}(r) + \frac{1}{r^3}A_m P_m^{'}(r)]P_n(r)rdr + k_o\int_0^1 H(r,\tau)\sum_{m=1}^{\infty}[A_m P_m(r)]P_n(r)rdr - g_o\int_0^1 H(r,\tau)\sum_{m=1}^{\infty}[A_m P_m^{''}(r) + \frac{1}{r}A_m P_m^{'}(r)]P_n(r)rdr - \mu_o^2 k_o\int_0^1 H(r,\tau)\sum_{m=1}^{\infty}[A_m P_m^{''}(r) + \frac{1}{r}A_m P_m^{'}(r)]P_n(r)rdr + \mu_o^2 g_o\int_0^1 H(r,\tau)\sum_{m=1}^{\infty}[A_m P_m^{iv}(r) + \frac{2}{r}A_m P_m^{'''}(r) - \frac{1}{r^2}A_m P_m^{''}(r) + \frac{1}{r^3}A_m P_m^{'}(r)]P_n(r)rdr + \int_0^1\sum_{m=1}^{\infty}[\frac{d^2A_m}{d\tau^2}P_m(r)]P_n(r)rdr - \mu_o^2\int_0^1\sum_{m=1}^{\infty}[\frac{d^2A_m}{d\tau^2}P_m^{''}(r) + \frac{1}{r}\frac{d^2A_m}{d\tau^2}P_m^{'}(r)]P_n(r)rdr - \int_0^1 q_o(r,\tau)P_n(r)rdr + \mu_o^2\int_0^1[q_o^{''}(r,\tau) + \frac{1}{r}q_o^{'}(r,\tau)]P_n(r)rdr - p_o(\tau)\int_0^1\delta(0)P_n(r)rdr - \sum_{m=1}^{\infty}\Big[A_m P_m^{'''}(r=1) + A_m P_m^{''}(r=1) - A_m P_m^{'}(r=1)\Big]P_n(r=1) + \sum_{m=1}^{\infty}[A_m P_m^{''}(r=1) + \nu A_m P_m^{'}(r=1)]P_n^{'}(r=1) + g_o\left[\frac{\partial w_f}{\partial r}_{r=1^+} - \sum_{m=1}^{\infty}\Big[A_m P_m^{'}(r=1)\Big]\right] \times H(r=1,\tau)P_n(r=1) = 0 \quad (20)$$

The differentiation with respect to r is denoted by the prime notation. Rearranging the above equation gives second-order nonlinear differential equation set which is the governing equation of the problem with respect to the non-dimensional time τ,

$$\sum_{m=1}^{\infty}\left[B_{nm}\frac{d^2A_m(\tau)}{d\tau^2} + C_{nm}(\tau)A_m(\tau)\right] = D_n(\tau) \quad n = 1, 3, 5, \ldots \quad (21)$$

where

$$B_{nm} = \int_0^1 P_n(r)P_m(r)rdr - \mu_o^2\int_0^1\left[P_n(r)P_m^{''}(r) + \frac{1}{r}P_n(\eta)P_m^{'}(r)\right]r\,dr$$

$$D_n(\tau) = \int_0^1 q_o(r,\tau)P_n(r)\,r\,dr + p_o(\tau)\int_0^1\delta(0)P_n(r)\,r\,dr - g_o\frac{\partial w_f}{\partial r}_{r=1^+}H(r=1,\tau)P_n(r=1)$$

$$C_{nm}(\tau) = \int_0^1\Big[P_m^{iv}(r) + \frac{2}{r}P_m^{'''}(r) - \frac{1}{r^2}P_m^{''}(r) + \frac{1}{r^3}P_m^{'}(r)\Big]P_n(r)\,r\,dr + k_o\int_0^1 H(r,\tau)P_m(r)P_n(r)\,r\,dr - g_o\int_0^1 H(r,\tau)\Big[P_m^{''}(r) + \frac{1}{r}P_m^{'}(r)\Big] \times P_n(r)\,r\,dr - \mu_o^2 k_o\int_0^1 H(r,\tau)\Big[P_m^{''}(r) + \frac{1}{r}P_m^{'}(r)\Big]P_n(r)\,r\,dr + \mu_o^2 g_o\int_0^1 H(r,\tau)\Big[P_m^{iv}(r) + \frac{2}{r}P_m^{'''}(r) - \frac{1}{r^2}P_m^{''}(r) + \frac{1}{r^3}P_m^{'}(r)\Big]P_n(r)\,r\,dr - \Big[P_m^{'''}(r=1) + P_m^{''}(r=1) - P_m^{'}(r=1)\Big]P_n(r=1) + \Big[P_m^{''}(r=1) + \nu P_m^{'}(r=1)\Big]P_n^{'}(r=1) - g_o H(r=1,\tau)P_m^{'}(r=1)P_n(r=1) \quad (22)$$

B_{nm} is related to inertial forces and can be accepted the mass matrix of the problem, although the mass per unit area of the plate m is not directly obvious in its terms, because it is included in the definition of non-dimensional time τ. The matrix D_n represents the effect of the external loads, and the matrix C_{nm} includes indirectly the bending stiffness of the plate and the foundation stiffness, where these stiffnesses are not seen directly, because they are included in the definition of the non-dimensional parameters. The matrix C_{nm} depends on time, because the Heaviside contact function defines the contact region boundary and introduces nonlinearity into the plate's response. As expected, the unilateral nature of the support—assuming that no tensile force can be transmitted between the plate and the foundation—has a significant impact on the overall behavior. The static and dynamic plate responses, which involve both forced and free vibrations, are determined by solving the governing differential Eqs. (21). The unilateral nature of the foundation leads to a system of nonlinear second-order equations with respect to time.

Typically, the plate's governing equation is formulated by analyzing the balance of internal moments and forces in an infinitesimal element, while also incorporating the effects of foundation reactions and inertia forces [1]. Furthermore, the equilibrium of global vertical forces can be derived from the free-body diagram of the entire plate, including all external forces, such as those resulting from inertia, as follows (Fig. 1(e)):

$$\begin{aligned} &P_o(t) + 2\pi \int_o^A Q_o(R,\, t)\, R\, dR \\ &= 2\pi K_o \int_o^A W(R,\, t)\, R\, dR - 2\pi G_o \int_o^A \left(\frac{\partial^2 W}{\partial R^2} + \frac{1}{R}\frac{\partial W}{\partial R} \right) R dR - \\ &- 2\pi A G_o H(R = A,\, t) \left[\left(\frac{\partial W_f}{\partial R} \right)_{R=A^+} - \left(\frac{\partial W}{\partial R} \right)_{R=A^-} \right] \\ &+ 2\pi m \int_o^A \frac{\partial^2 W}{\partial t^2}\, R\, dR \end{aligned} \tag{23}$$

where in the left-hand side of the equation sign, the terms relate to the distributed load $Q_o(R,\, t)$ and the external concentrated load $P_o(t)$. The terms in the right-hand side address to the foundation reaction due to the springs and to the membrane stiffnesses, $P_w(t)$ and $P_g(t)$, respectively. The total foundation reaction consists of as $P_f(t) = P_w(t) + P_g(t)$. The final component $P_i(t)$ denotes the resultant of the inertia forces. The term before last term denotes the unbalanced component of the membrane tension $P_p(t)$ at the edge of the plate, which emerges due to the discontinuity of the slope of the membrane at the edge. The overall equilibrium of the forces can be written using the non-dimensional parameters:

$$p_o(\tau) + 2\pi \int_o^1 q_o(r,\, \tau)\, r\, dr = p_w(\tau) + p_g(\tau) + p_p(\tau) + p_i(\tau) \tag{24}$$

where

$$p_w(\tau) = 2\pi k_o \sum_{m=1}^{\infty} \left[A_m(\tau) \int_o^1 P_m(r)\, r\, dr \right].$$

$$p_g(\tau) = -2\pi g_o \sum_{m=1}^{\infty} \left[A_m(\tau) \int_o^1 \left[P_m''(r) + \frac{1}{r} P_m'(r) \right] r\, dr \right].$$

$$\begin{aligned} p_p(\tau) &= -2\pi g_o H(r = 1,\, \tau) \left[\left(\frac{\partial w_f(r)}{\partial r} \right)_{r=1^+} \right. \\ &\quad \left. - \sum_{m=1}^{\infty} \left[A_m(\tau) P_m'(r) \right]_{r=1} \right] \\ p_i(\tau) &= 2\pi \sum_{m=1}^{\infty} \left[\frac{\partial^2 A_m(\tau)}{\partial \tau^2} \int_o^1 P_m(r)\, r\, dr \right] \end{aligned} \tag{25}$$

In the above equations $W_f(R,\, T) = A\, w_f(r,\, \tau)$ shows the surface of the foundation outside the contact point, i.e., $R_{contact} \le R < \infty$, i.e., $r_{contact} \le r < \infty$ which appear as the solution of the following differential equation

$$\begin{aligned} &K_o W_f(R,\, t) - G_o \left(\frac{\partial^2 W_f}{\partial R^2} + \frac{1}{R}\frac{\partial W_f}{\partial R} \right) = 0 \\ &W_f(R,\, t) = A\, w_f(r,\, \tau) = A\, F(\tau) \overline{K}_o(s_o r) \end{aligned} \tag{26}$$

where $F(\tau)$ is a function of time only which controls time variations of the foundation surface, $\overline{K}_o(s_o r)$ is the modified Bessel function of the second kind and $s_o = \sqrt{k_o/g_o}$, where A/s_o corresponds to the characteristic length of the foundation and it is related directly to the nonlocal property of it. Two-dimensional foundation model approaches Winkler model as $s_o \to \infty$.

5 Numerical Treatment

The numerical treatment of the problem involves solving the nonlinear system of Eqs. (21) for static loading, as well as solving the system of the nonlinear second-order differential equations for the dynamic case, including the associated initial conditions. For static loading, iterations are performed for the contact region until an acceptable level of accuracy is achieved. Specifically in the case of $r_{contact} = R_{contact}/A < 1$, a contact radius is assumed numerically; the stiffness matrix C_{nm} and the loading vector D_n are evaluated using Gaussian quadrature procedure.

It is important to note that as a requirement of assumption the last term of the loading vector D_n in Eq. (25) vanishes, i.e., the unbalanced component of the surface tension G_o does not arise, because the complete contact and discontinuity on the slope of the membrane do not exist. Having determined the constants of the displacement functions A_n from the governing equation, the displacement function and following the lift-off and the contact conditions (11) the contact radius determined and compared with the one assumed. If necessary, the accuracy of the result related to the contact radius can be improved by continuing the iteration procedure updating contact radius $r_{contact}$ and contact function $H(r)$ accordingly. In the present case, since the numerical solution is obtained as the gradual change of a specific parameter for the graphical representation, obtaining an acceptable result in iteration did not present a significant difficulty. However, it is clear that a more meticulous iteration would be required for a complex change in the loading. In the case of complete contact, i.e., $r_{contact} = R_{contact}/A = 1$, the last term of the loading vector D_n in Eq. (25) has to be evaluated and included to the loading vector D_n. In this case, the slope of the foundation surface at the plate edge can be evaluated from Eq. (25) as $dw_f(r = 1)/dr = -F(\tau)\, s_o \overline{K}_1(s_o)$ by assuming a numerical value for F. The constants of the displacement functions A_n from the governing equation are determined, and the assumption for F is checked by requiring that the vertical displacement of the plate edge is equal considering the free foundation surface and the foundation surface at the plate.

$$\begin{aligned} W_f(A) &= A\, w_f(1) = \mathrm{AF} K_o(s_o) \\ &= W(A) = A\, w(1) \\ &= A \sum_{m=1}^{\infty} \sum_{n=1}^{\infty} A_m P_m(1) \end{aligned} \tag{27}$$

In this case, if necessary, the approximation of F can be improved by continuing to the iteration procedure. Since static problem is considered, the time dependency vanishes in the above equations. As explained above for the partial contact case, i.e., $r_{contact} < 1$, iteration is carried out for $r_{contact}$; however, the complete contact case $r_{contact} = 1$; the iteration processes are required for the constant F.

When the dynamic problem is considered, the numerical treatment begins by determining the initial conditions, which can be evaluated as explained in the static case above. After the plate's initial configuration and the foundation surface are established, the numerical solution can proceed in the time direction. This is done by solving the system of the second-order differential Eqs. (21) along the time direction using the contact radius $r_{contact}(\tau)$ and the parameter of the free base surface $F(\tau)$ from the previous time step. The accuracy of the iteration process can be verified by varying the time step. The numerical findings require the Chebyshev polynomials to be integrated, including the contact function $H(r, \tau)$. Numerical integrations are performed using the Gaussian quadrature rule, with a limited number of terms. A series of simulations is carried out to identify the number of terms required to achieve satisfactory numerical accuracy. These involve varying the truncation levels of the series and adjusting Gauss integration point numbers. The resulting data are presented graphically to assess the accuracy of the proposed method. It was found that using 20 Gaussian integration points and considering four terms (i.e., $m = 1, 3, 5, 7$) provided results with satisfactory accuracy for the graphical representations. In solving the system of differential equations, acceptable accuracy is achieved by employing the standard constant acceleration method.

Following the determination of the constants of displacement function A_n of the plate, all variables of the foundation and the plate, i.e., the foundation reactions due to the stiffnesses k_o and g_o, the reaction force at the edge of the plate along its periphery in complete contact case and the shear force and bending moment of the plate, can be evaluated easily. To assess the influence of accumulated numerical errors in the dynamic analysis, results from numerical integration with varying time step sizes are compared. It is well known that reducing the time step in the solution of the differential Eq. (21) can often improve the accuracy of the results, especially for linear systems. However, this is not always guaranteed for nonlinear systems, as is the case in the present analysis. Numerical results provide valuable insights into the plate behavior under static and dynamic loads, especially when considering a broad range of the non-dimensional variables. However, for the sake of brevity, only a limited number of results are presented.

A straightforward examination of the free vibrations for a completely free rigid plate resting on a conventional two-parameter foundation can be expressed by including the vertical component of the surface tension along the periphery of the plate (Fig. 1e).

$$\begin{aligned} P_o(t) + \pi A^2 Q_o(t) = {} & \pi A^2 m \frac{d^2 W_o(t)}{dt^2} \\ & - 2\pi G_o A \frac{\partial W_f(R = 1, t)}{\partial R} \\ & + \pi A^2 K_o W_o(t) \end{aligned} \tag{28}$$

which yields by using the non-dimensional parameters

$$\frac{d^2 w_o(\tau)}{d\tau^2} + \pi [k_o + \frac{\overline{K}_1(s_o)}{\overline{K}_o(s_o)} 2 s_o g_o] w_o(\tau) = p_o(\tau) + \pi q_o(\tau) \tag{29}$$

This represents the equation of motion for the single degree of freedom system, which provides the non-dimensional circular frequency of the free vibration and the translatory static displacement, assuming the loads are static.

$$\omega_o^2 = \pi \left[k_o + \frac{\overline{K}_1(s_o)}{\overline{K}_o(s_o)} 2 s_o g_o \right] \quad w_{\text{static}} = \frac{p_o/\pi + q_o}{k_o + \frac{\overline{K}_1(s_o)}{\overline{K}_o(s_o)} 2 s_o g_o} \tag{30}$$

where $\overline{K}_o(s_o)$ and $\overline{K}_1(s_o)$ are the modified Bessel functions of the second kind.

Once again, it should be noted that this analysis strongly emphasizes the use of non-dimensional variables associated with time, loading, and geometry to guarantee the broad applicability of the numerical results and conclusions. The displacements and the circular frequencies obtained for the rigid plate are employed to check the numerical solution in general, especially for the plate with high bending stiffness relative to the spring stiffness of the foundation, where a dominant rigid displacement of the plate is expected.

6 Numerical Results

MATLAB [58] is used to carry out the numerical analysis. A systematic investigation is performed to evaluate how several plate and foundation variables influence the system's behavior. The results are presented in comparative graphical form to highlight these effects. Leissa [59] presents extensive treatment and numerical results concerning the free vibration of plates with various boundary conditions and shapes, including the circular plates with completely free support conditions. In the present study, properties of Chebyshev polynomials and Bessel functions, along with their derivatives, are utilized based on the textbooks of Mason and Handscomb [56] and MacLachlan [60]. Additionally, SAP2000 software [51] is employed to validate some of the numerical results of this study, specifically for both conventional and unilateral Winkler foundation properties, which represent a special case of the two-parameter foundation approach. In the application of SAP2000 software to be compatible with the present analysis, thin plate assumed where the transverse shear deformation is neglected. Specifically, the 'shell-thin' element formulation was employed to represent the Kirchhoff plate behavior. A free plate resting on an elastic foundation was considered. To implement the unilateral (tensionless) nature of the contact, the foundation was modeled using compression-only (gap) link elements at the mesh nodes, ensuring that reaction forces are generated only under downward displacement. Since the program runs by using dimensional quantities, the solution is obtained by selecting dimensional quantities that match the dimensionless quantity chosen for the geometry, load, elastic material, and elastic foundation parameters. After testing with various element numbers, 20 and 24 elements are adopted in the radial and circumferential directions, respectively. The choice of element numbers was influenced by the accuracy required to determine the separation point in case the plate separates from the foundation.

Furthermore, the results for rigid circular plate, i.e., the static displacement and free vibration periods, are used to validate the results of the elastic plate. These results are provided in conjunction with the current findings to facilitate comparison. The resulting data are presented graphically to assess the accuracy of the proposed method.

The accuracy of the numerical study is influenced by the number of Chebyshev polynomials, the number of Gaussian integration points, and the time step interval used in the dynamic solution. The selection of these parameters was made by comparing static and dynamic results for various values given to these three parameters. After numerous numerical solutions, it was found that using 20 Gaussian integration points, considering four Chebyshev polynomials (i.e., $m = 1, 3, 5, 7$) and assuming the time step $\Delta\tau = 0.1$, the numerical solutions can be obtained with satisfactory for the graphical representations. In solving the system of differential equations, acceptable accuracy is achieved by employing the standard constant average acceleration method which is a special case of the Newmark's method assuming $\gamma = 1/2$ and $\beta = 1/4$ [61]. This implicit scheme is known for its favorable stability properties and energy preservation characteristics in structural dynamics. It is obvious that these values depend on the spatial and time-dependent variations of the loading, and that in complex loading situations, the same accuracy can be obtained by considering more Chebyshev polynomials and integration points and smaller time steps.

Figure 2 shows variations in the displacement of the edge of the plate $w_a(k_o) = w(r = 1, k_o)$, the displacement of the center of the plate $w_o(k_o) = w(r = 0, k_o)$, and the contact radius $r_{contact}(k_o)$, for different load q_o/p_o values of the plate as a function of the spring stiffness of the foundation k_o. The global force equilibrium, i.e., $p_f(k_o) = p_o + \pi q_o$, is checked for all static loading cases to validate the numerical results. In the numerical solution, q_o is assumed to be uniformly distributed. As expected, while the full contact of the plate occurs at low values of the spring stiffness of the foundation k_o, an increase in the stiffness initiates a lift-off region at the edge of the plate, which progresses toward the center. The figure illustrates that as the load q_o increases, the lift-off region is suppressed, and the contact region expands. As is well known, the contact radius does not depend on the external load level when the plate is subject to a single

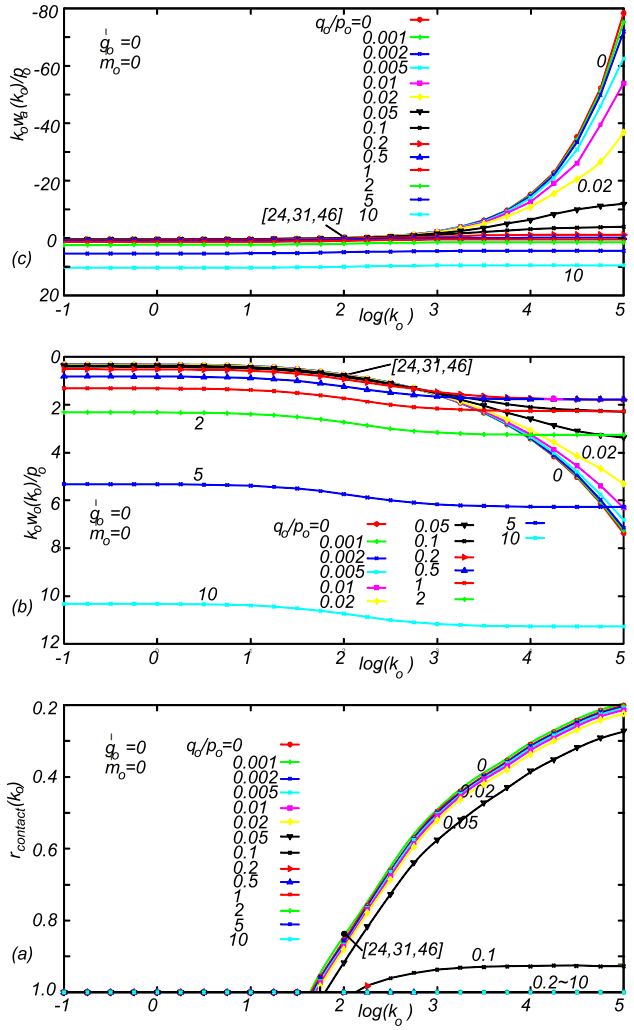

Fig. 2 Variations of **a** the contact radius $r_{contact}(k_o)$, **b** the displacement of the center of the plate $k_o w_o(k_o)/p_o$, and **c** the displacement of the edge of the plate $k_o w_a(k_o)/p_o$, for various values the load q_o of the plate as a function the spring stiffness of the foundation k_o

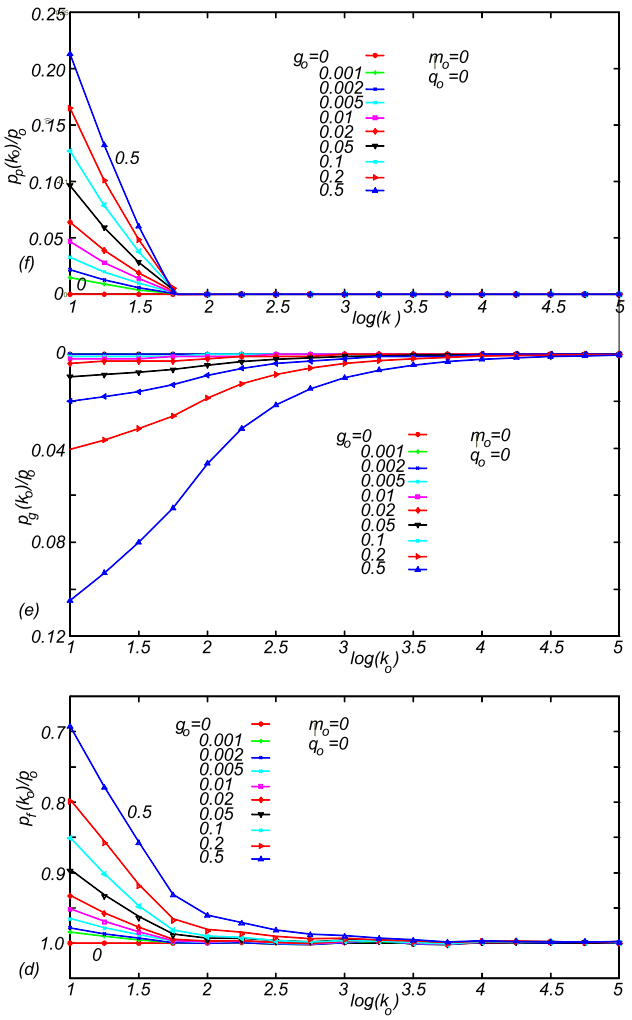

Fig. 3 Variations of **a** the contact radius $r_{contact}(k_o)$, **b** the displacement of the center of the plate $k_o w_o(k_o)/p_o$, **c** the displacement of the edge of the plate $k_o w_a(k_o)/p_o$, **d** the total reaction of the foundation $p_f(k_o)/p_o$, **e** the foundation reaction $p_g(k_o)/p_o$ due to the membrane foundation stiffness, and f) the foundation reaction $p_p(k_o)/p_o$ at the edge of the plate due to the membrane stiffness g_o for various values of the membrane stiffness g_o as a function the spring stiffness of the foundation k_o

type of loading, i.e., p_o. However, displacements vary linearly with the loading level, i.e., the displacements of the plate, $w_o(k_o)$ and $w_a(k_o)$, are linearly related to the loading level, p_o. An increase in the applied load increases the displacements proportionally without altering the lift-off region, thereby maintaining vertical force equilibrium. Conversely, the lift-off region depends on the loading ratio when two types of loading are involved, i.e., on q_o/p_o. However, this linear relationship does not hold when multiple loading types are applied. In such cases, the linearity breaks down. A comparison of the displacement variations shows that as stiffness decreases, the displacements approach those of a rigid plate or a very flexible foundation, which serves as validation for the current analysis, i.e., $k_o w_o(k_o \to 0) \approx k_o w_a(k_o \to 0) \approx q_o + p_o/\pi$. Notably, a more pronounced change is observed for larger values of the foundation stiffness k_o.

Figure 3 displays variations in the contact radius $r_{contact}(k_o)$, the displacement of the center of the plate $w_o(k_o)$, displacement of the edge of the plate $w_a(k_o)$, the total foundation reaction $p_f(k_o)$, the foundation reaction $p_g(k_o)$ due to the membrane foundation stiffness g_o, and the foundation reaction $p_p(k_o)$ at the plate edge due to the membrane stiffness g_o, all as a function of membrane stiffness g_o relative to the spring stiffness of the foundation k_o. The total foundation reaction $p_f(k_o) = p_w(k_o) + p_g(k_o)$ consists of the reaction applied to the bottom surface of the plate, resulting from both the spring k_o and the membrane stiffness g_o. In this case, the global force equilibrium is also checked, $p_f(k_o) + p_p(k_o) = p_o$ which serves as validation

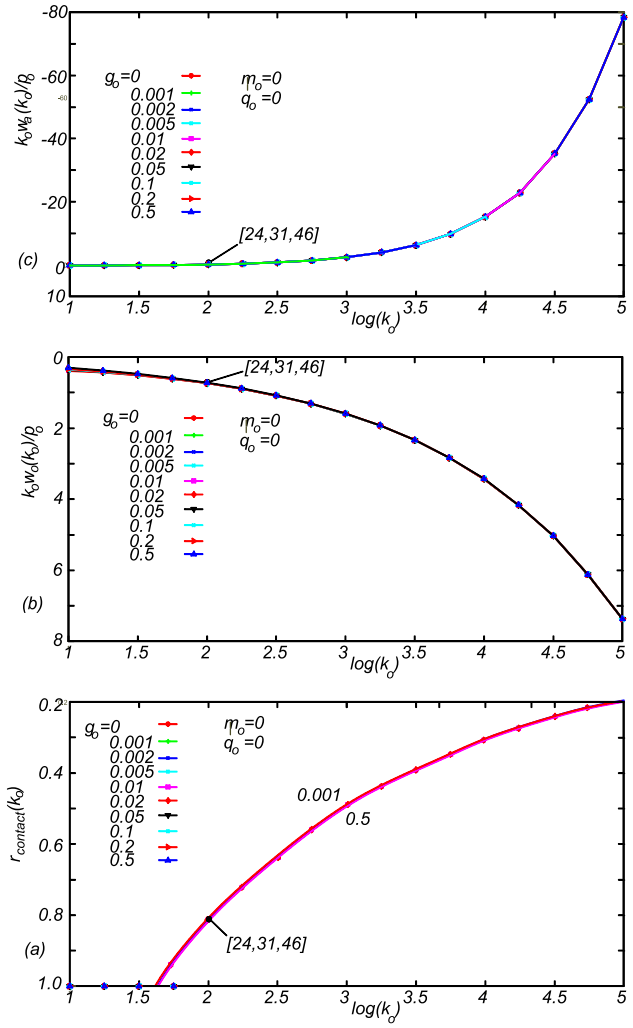

Fig. 3 continued

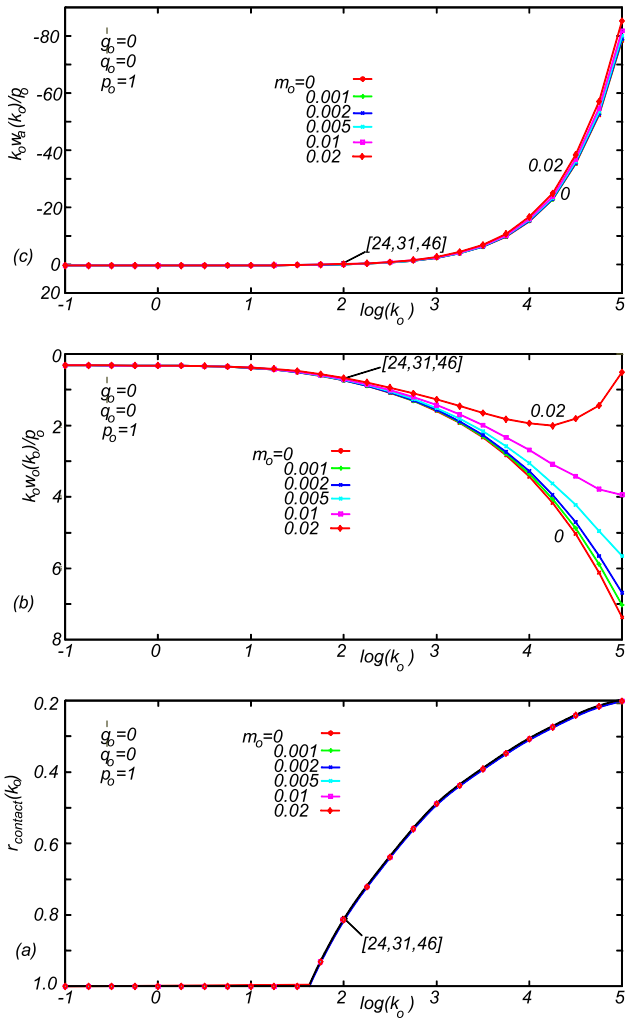

Fig. 4 Variations of **a** the contact radius $r_{contact}(k_o)$, **b** the displacement of the center of the plate $k_o w_o(k_o)/p_o$, and c) the displacement of the edge of the plate $k_o w_a(k_o)/p_o$, for various values of the non-local parameter of the plate m_o as a function the spring stiffness of the foundation k_o

for the numerical results. Inspection of the figures reveals that the variations in the contact radius and displacements are relatively insensitive to the membrane stiffness within the examined numerical range, while the foundation reactions, $p_f(k_o)$, $p_g(k_o)$, and $p_p(k_o)$, show significantly different variations. The foundation reaction $p_p(k_o)$ occurs when full contact is established and disappears in partial contact case as seen in Fig. 1e, indicating that the foundation is relatively flexible.

Figure 4 illustrates variations in the displacement of the plate edge $w_a(k_o)$, the displacement of the center of the plate $w_o(k_o)$, and the contact radius $r_{contact}(k_o)$, for different values of the non-local parameter $m_o = \mu_o^2$ as a function of the spring stiffness of the foundation k_o. Here too, the global force equilibrium is checked as, $p_f(k_o) = p_o + \pi q_o$, i.e., which can be regarded as validation for the numerical results. Furthermore, for a very flexible foundation $k_o w_o(k_o \to 0) \approx k_o w_a(k_o \to 0) \approx q_o + p_o/\pi$ is satisfied as well. The foundation reactions $p_g(k_o)$ and $p_p(k_o)$ disappear in this case, because of the assumption $g_o = 0$. Inspection of the figures indicates that the variations in contact radius $r_{contact}(k_o)$ and the edge displacements $w_a(k_o)$ are not very sensitive to the non-local parameter $m_o = \mu_o^2$ within the numerical range considered. However, the central displacement of the plate $w_o(k_o)$ shows different variations as the foundation spring stiffness k_o increases. Figures 2, 3, and 4 include results from the previous studies [24, 31] for verification purposes, as well as the results obtained using the finite analysis software SAP2000. As can be observed, these results align closely with the numerical results of the present study.

In the analysis presented, arbitrary time variations for the external loads can be considered, provided that $p_o(\tau)$ is applied at the center of the plate and $q_o(r, \tau)$ has a rotational symmetry. However, for simplicity, a specific time function is employed in the numerical analysis, assuming

that $q_o(\tau)$ is uniformly distributed. Furthermore, the circular plate is considered to be initially in equilibrium under static loads without any initial velocity at $\tau = 0$. Then the loads, p_o and q_o, are suddenly changed to $b_o p_o$ and $b_o q_o$, respectively, for $\tau > 0$, where $b_o < 1$ and $b_o > 1$ correspond to sudden decreases (unloading) and increases (loading), respectively. For all remaining numerical analysis $p_o = 1$ is assumed. Figure 5 displays results for $k_o = 1000$ and $q_o = g_o = m_o = 0$, Fig. 6 for $m_o = 0.02$ and $q_o = 0.1$ and $g_o = m_o = 0$, Fig. 7 for $k_o = 10$ and $g_o = 0.1$ and $q_o = m_o = 0$, and Fig. 8 for $k_o = 1000$ and $m_o = 0.02$ and $q_o = g_o = 0$. The spring stiffness of the foundation k_o is chosen specifically to reveal clearly the effect of the nonzero parameter. Numerical results for $b_o = 0.5$ and $b_o = 1.5$ correspond to the loading cases where the load is decreased by 50% and increased by 50%, respectively.

Figures 5a, 6a, and 8a display the time variations of the contact radius $r_{contact}(\tau)$. The time variation is not shown for $k_o = 10$ in Fig. 7, because full contact is established in this case, i.e., $r_{contact}(\tau) = 1$ due to the relatively soft foundation. As expected, nonlinearity emerges when partial contact occurs due to the unilateral property of the foundation, leading to a lift-off. Figures 5b, 6b, 7a, and 8b show the time variations of the center of the plate $w_o(\tau)$, while Figs. 5c, 6c, 7b, and 8c display those of the edge of the plate $w_a(\tau)$. In the dynamic analysis, the contact radius is updated at each time step in performing the numerical solution. Since a continuous variation is involved, and the global force balance by including the inertia force is checked at each step, the chosen time step ensured that sufficient results are obtained. An inspection of the figures reveals that nonlinearity is more pronounced in the variations of the contact radius, while it appears less significant in the displacements. Figures 5d, 6d, 7c, and 8d present the time variations of the total foundation reaction $p_f(\tau) = p_w(\tau) + p_g(\tau)$. Figures 5e, 6e, 7f, and 8e show the time variations of the inertia. Comparison of Figs. 5a and 6a shows that the presence of a uniformly distributed load q_o reduces the lift-off of the plate and suppresses the nonlinear behavior. Displacement variations are relatively larger in the unloading case $b_o = 0.5$ compared to the loading case $b_o = 1.5$, because the separation of the plate is more significant during unloading than during loading. The separation region expands during unloading, decreasing the global foundation stiffness, which in turn increases the nonlinear behavior of the plate. Conversely, during loading, the expansion of the contact area reduces nonlinearity.

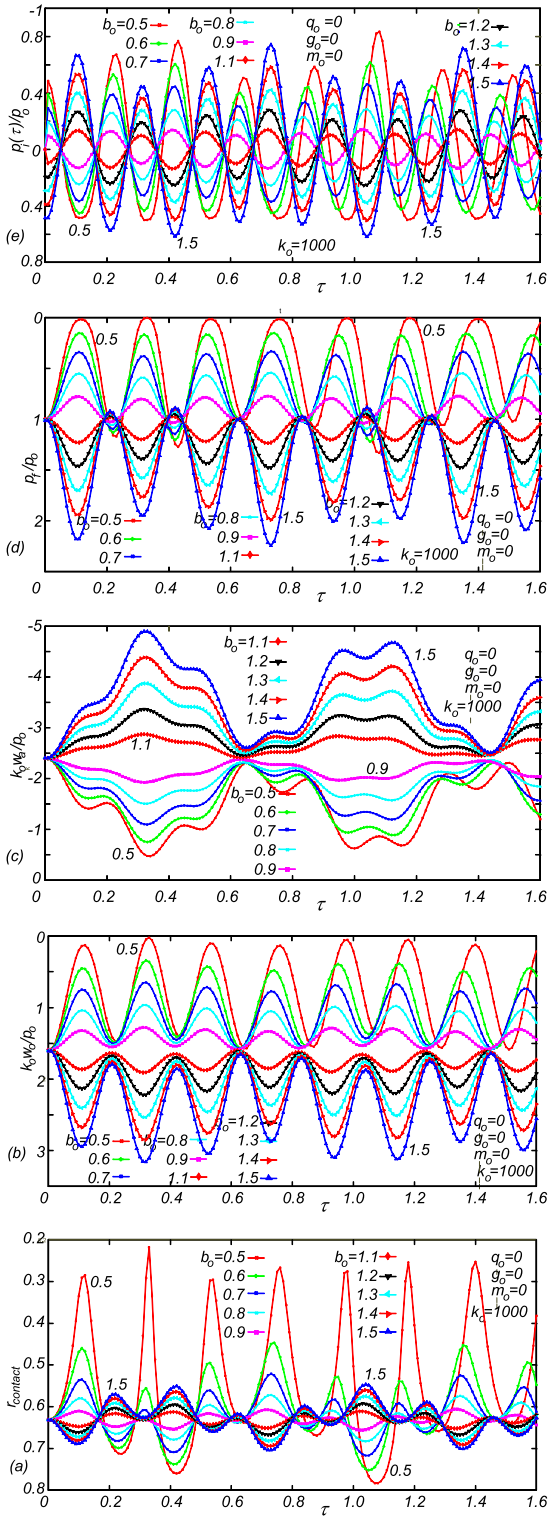

Fig. 5 Time variation of **a** the contact radius $r_{contact}(\tau)$, **b** the displacement of the center of the plate $k_o w_o(\tau)/p_o$, **c** the displacement of the edge of the plate $k_o w_a(\tau)/p_o$, **d** the total reaction of the foundation $p_f(\tau)/p_o$, and **e** the total inertia force of the plate $p_i(t)/p_o$ for the loading ($b_o < 1$) and the unloading ($b_o > 1$) cases assuming $k_o = 1000$

7 Conclusions

In this research, the behavior of a circular plate under both uniformly distributed and concentrated loads is explored in terms of its static and dynamic characteristics. The plate is

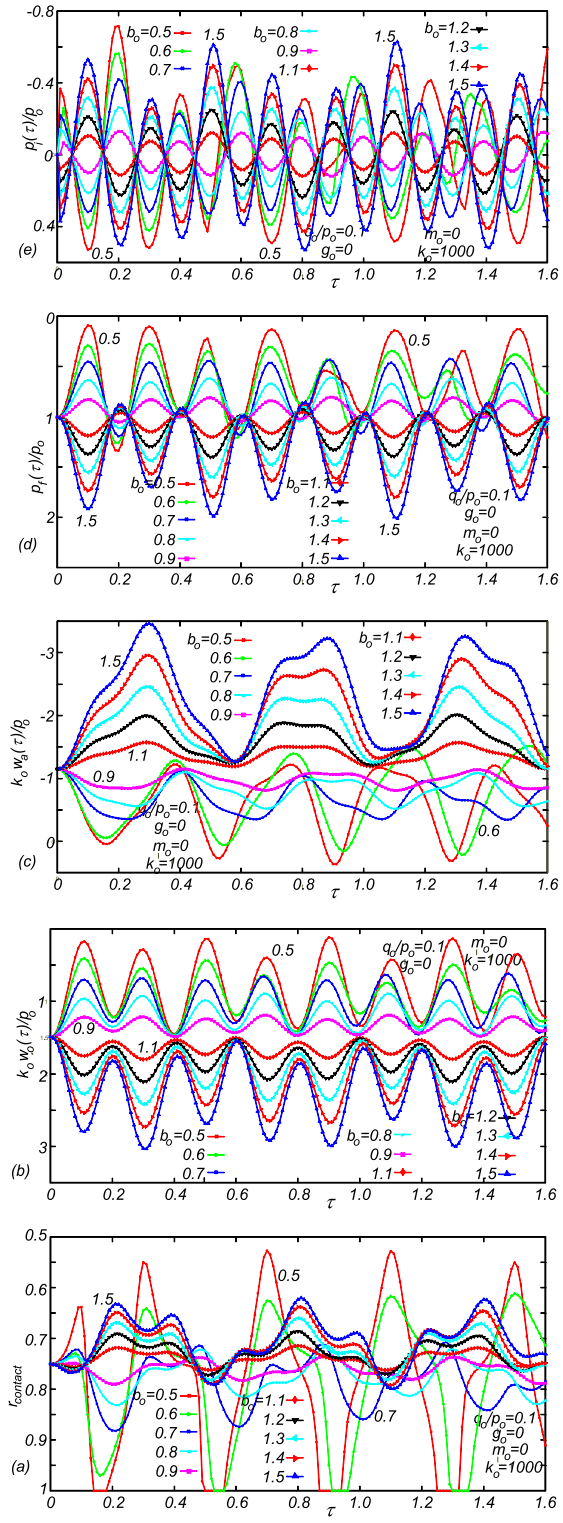

Fig. 6 Time variation of **a** the contact radius $r_{contact}(\tau)$,**b** the displacement of the center of the plate $k_o w_o(\tau)/p_o$, **c** the displacement of the edge of the plate $k_o w_a(\tau)/p_o$, **d** the total reaction of the foundation $p_f(\tau)/p_o$, and **e** the total inertia force of the plate $p_i(t)/p_o$ for the loading ($b_o < 1$) and the unloading ($b_o > 1$) cases assuming $k_o = 1000$ and $q_o = 0.1$

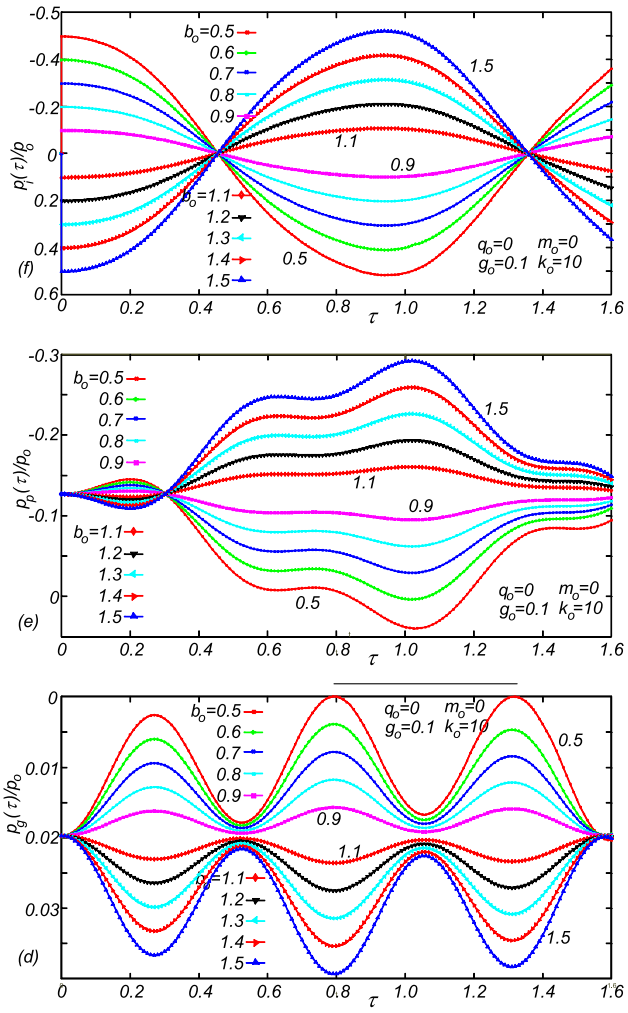

Fig. 7 Time variation of **a** the displacement of the center of the plate $k_o\, w_o(\tau)/p_o$, **b** the displacement of the edge of the plate $k_o w_a(\tau)/p_o$, **c** the total reaction of the foundation $p_f(\tau)/p_o$, **d** the total reaction of the foundation $p_g(\tau)/p_o$, **e** the total reaction of the foundation $p_p(\tau)/p_o$ at the edge of the plate due to the membrane stiffness g_o, and f) the total inertia force of the plate $p_i(t)/p_o$ for the loading ($b_o < 1$) and the unloading ($b_o > 1$) cases assuming $k_o = 10$ and $g_o = 0.1$

assumed to possess non-local properties and supported by a unilateral two-parameter foundation. The two-parameter foundation used in this study can be considered a non-local generalization of the conventional Winkler foundation model. Consequently, the study accounts for both the linear non-local properties of the plate and the foundation. As in the conventional two-parameter foundation model, the governing equation of the non-local plate and the foundation reaction are linear. However, the unilateral foundation model gives rise to complex nonlinear behavior. The governing equation is achieved by applying Galerkin approach whereas a series of Chebyshev polynomials are used to express the displacement field. For the dynamic case, where the inertia forces of the plate mass are considered, a system of nonlinear

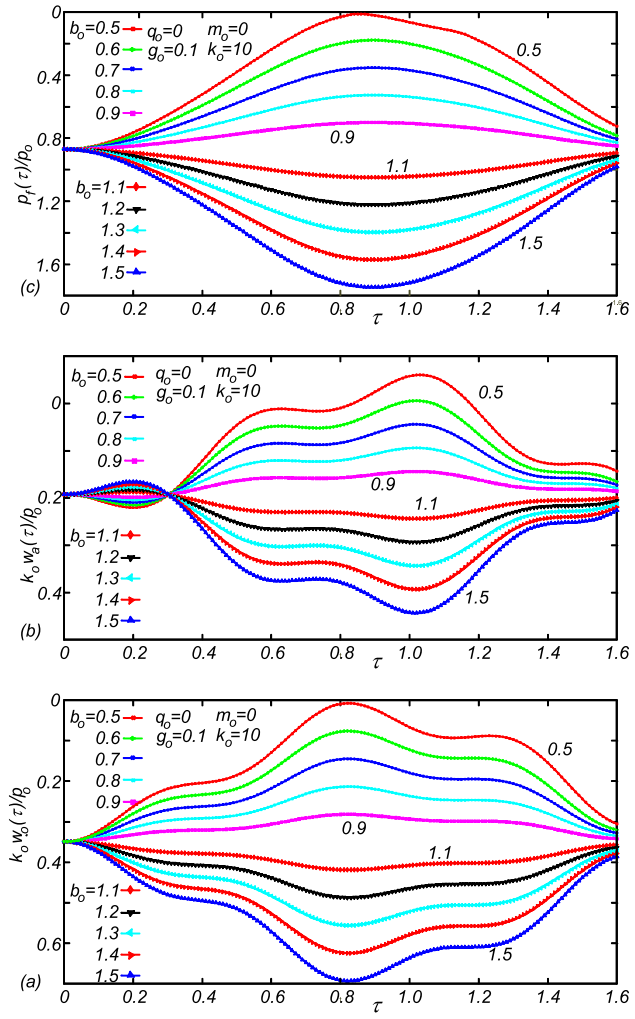

Fig. 7 continued

second-order differential equations is obtained. This equation simplifies into a system of nonlinear algebraic equations when the load is static.

In the analysis, the unilateral foundation property is incorporated by adding a supplementary contact function. During static analysis, the function is evaluated iteratively. During the dynamic analysis, this function is recalculated continuously at every time step after evaluating the initial condition. Due to the variation in the circular contact area, the vertical stiffness of the plate changes. Accordingly, the stiffness matrix is recalculated in every step of time. The stiffness matrix elements are having integration within the contact region, making them indirectly time-dependent. The derivation of the governing equation is done with special attention. In order to encompass diverse variables within graphical visualizations, non-dimensional parameters are used. The net balance of forces acting in the direction perpendicular to the plate surface is obtained comprehensively to check the numerical solution. Furthermore, particular focus is placed

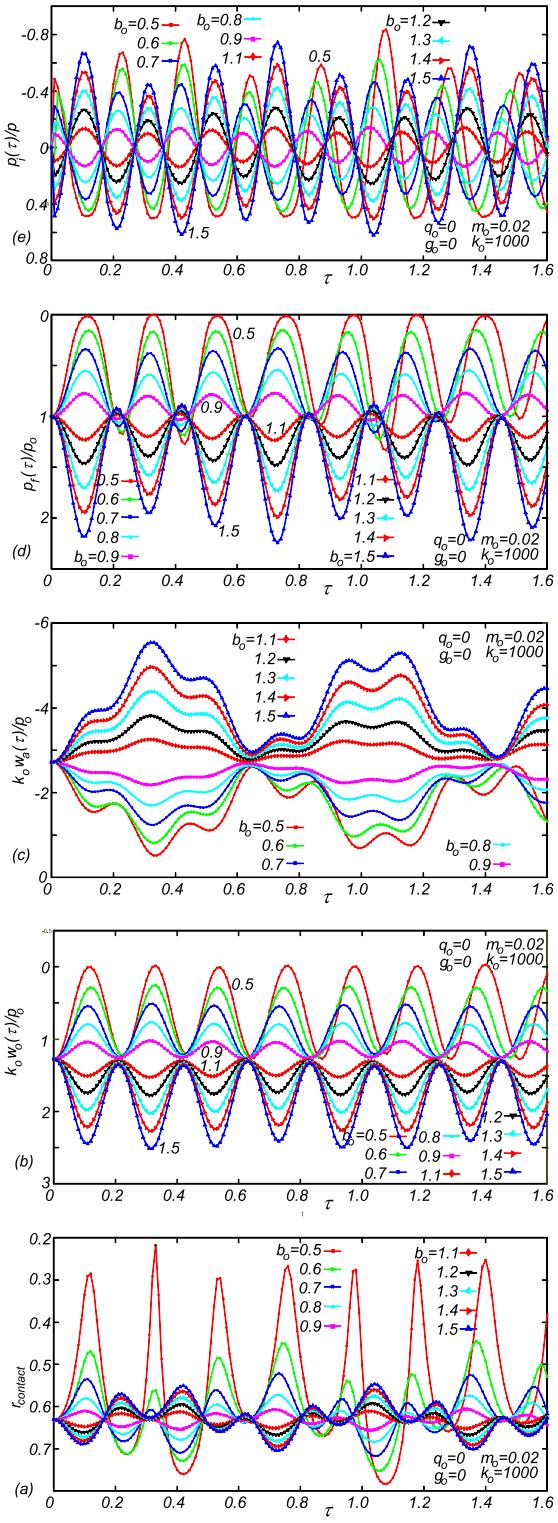

Fig. 8 Time variation of **a** the contact radius $r_{contact}(\tau)$, **b** the displacement of the center of the plate $k_o\, w_o(\tau)/p_o$, **c** the displacement of the edge of the plate $k_o w_a(\tau)/p_o$, **d** the total reaction of the foundation $p_f(\tau)/p_o$, and **e** the total inertia force of the plate $p_i(t)/p_o$ for the loading ($b_o < 1$) and the unloading ($b_o > 1$) cases assuming $k_o = 1000$ and $m_o = 0.02$

on the foundation reaction in the two-parameter foundation approach, which consists of two parts. One part is the distributed reaction from the foundation applied to the bottom surface of the plate, which generalizes the Winkler model by including the first and second radial derivatives of the foundation surface in the rotationally symmetric case. The second part, rarely addressed in previous studies, arises in cases of complete contact at the edges of the plate where the slope of the foundation exhibits discontinuity. This part is linearly proportional to the discontinuity and the membrane stiffness of the foundation.

Numerical results are obtained via an iterative method for the contact radius and the shape function of the foundation surface beyond the contact region. The equilibrium of vertical force is derived from the free-body diagram of the plate, which validates the implementation of the numerical solution procedure for both the static and dynamic loadings. In dynamic simulation, the time step is chosen to achieve acceptable accuracy in the graphical visualizations of the numerical results. Although the analysis is based on arbitrarily varying time-dependent rotationally symmetric loads, both a central force and a uniformly distributed load are considered. The dynamic event is assumed to occur with a sudden, stepwise change in external loads. Time variations of the contact radius, as well as the central and edge displacements of the plate, foundation reactions, and inertia forces, are specifically presented. The inertia force is evaluated solely to check the equilibrium of vertical forces in the dynamic loading. The main contributions of this study can be summarized as follows: combination of nonlocal properties of the foundation and plate, condition of the separation of the plate from the foundation and extensive numerical results which display the static and dynamic behavior of the plate and effects of the nonlocality parameters on the solutions. Key conclusions are as follows:

a. A uniformly distributed load suppresses the lift-off of the plate and mitigates the nonlinearity of the problem, both in static and dynamic cases.
b. The computational findings reveal that nonlinearity is most significant in the changes of contact radius, especially when compared to the displacements of the plate. Meanwhile, a moderate level of nonlinearity appears in the plate's displacement behavior under partial contact conditions.
c. The effects of the plate and the non-local foundation parameters are relatively small within the numerical range considered in this study.
d. As the area of contact increases, the foundation exhibits greater stiffness in comparison with the plate. Yet, this contact area is not governed by the load's magnitude, but rather by the relative proportions of multiple applied forces. It does not depend on the loading level when only one type of loading is used.
e. The two-parameter foundation model exhibits two types of foundation reactions. One is applied to the bottom surface of the plate and is considered a distributed property, as typically seen in related studies. The second, often overlooked, arises in cases of complete contact, occurring at the free edges of the plate where the foundation surface exhibits slope discontinuity. When the edge of the plate is supported, this reaction appears as part of the support reaction.

Funding Open access funding provided by the Scientific and Technological Research Council of Türkiye (TÜBİTAK).

Data Availability The datasets generated during and/or analyzed during the current study are available from the corresponding author on reasonable request.

References

1. Timoshenko, S.; Woinowsky-Krieger, S.: Theory of Plates and Shells. McGraw-Hill, Auckland (1959)
2. Kerr, A.D.: Elastic and viscoelastic foundation models. J. Appl. Mech. **31**, 491–498 (1964). https://doi.org/10.1115/1.3629667
3. Kerr, A.D.: On the derivation of well posed boundary value problems in structural mechanics. Int. J. Solids Struct. **12**, 1–11 (1976). https://doi.org/10.1016/0020-7683(76)90069-X
4. Kerr, A.D.; Soicher, N.E.: A peculiar set of problems in linear structural mechanics. Int. J. Solids Struct. **33**, 899–911 (1996). https://doi.org/10.1016/0020-7683(95)00078-O
5. Weitsman, Y.: On the unbonded contact between plates and an elastic half space. J. Appl. Mech. **36**, 198–202 (1969). https://doi.org/10.1115/1.3564607
6. Weitsman, Y.: On foundations that react in compression only. J. Appl. Mech. **37**, 1019–1030 (1970). https://doi.org/10.1115/1.3408653
7. Kamiya, N.: Circular plates resting on bimodulus and no-tension foundations. J .Eng. Mech. Div. **103**, 1161–1164 (1977). https://doi.org/10.1061/JMCEA3.0002303
8. Villaggio, P.: A free boundary value problem in plate theory. J. Appl. Mech. **50**, 297–302 (1983). https://doi.org/10.1115/1.3167035
9. Dempsey, J.P.; Keer, L.M.; Pate, N.B.; Glasser, M.L.: Contact between plates and unilateral supports. J. Appl. Mech. **51**, 324–328 (1984). https://doi.org/10.1115/1.3167620

10. Dempsey, J.P.; Li, H.: Rectangular plates on unilateral edge supports: Part 1—theory and numerical analysis. J. Appl. Mech. **53**, 146–150 (1986). https://doi.org/10.1115/1.3171702
11. Dempsey, J.P.; Li, H.: Rectangular plates on unilateral edge supports: Part 2—implementation; concentrated and uniform loading. J. Appl. Mech. **53**, 151–156 (1986)
12. Li, H.; Dempsey, J.P.: Unbonded contact of a square plate on an elastic half-space or a Winkler foundation. J. Appl. Mech. **55**, 430–436 (1988). https://doi.org/10.1115/1.3173694
13. Ascione, L.; Grimaldi, A.: Unilateral contact between a plate and an elastic foundation. Meccanica **19**, 223–233 (1984). https://doi.org/10.1007/BF01743736
14. Kocatürk, T.: Rectangular anisotropic (orthotropic) plates on a tensionless elastic foundation. Mech. Compos. Mater. **31**, 277–284 (1995). https://doi.org/10.1007/BF00615642
15. Akbarov, S.D.; Kocatürk, T.: On the bending problems of anisotropic (orthotropic) plates resting on elastic foundations that react in compression only. Int. J. Solids Struct. **34**, 3673–3689 (1997). https://doi.org/10.1016/S0020-7683(96)00227-2
16. Hong, T.; Teng, J.G.; Luo, Y.F.: Axisymmetric shells and plates on tensionless elastic foundations. Int. J. Solids Struct. **36**, 5277–5300 (1999). https://doi.org/10.1016/S0020-7683(98)00228-5
17. Silva, A.R.D.; Silveira, R.A.M.; Gonçalves, P.B.: Numerical methods for analysis of plates on tensionless elastic foundations. Int. J. Solids Struct. **38**, 2083–2100 (2001). https://doi.org/10.1016/S0020-7683(00)00154-2
18. Wang, Y.H.; Tham, L.G.; Cheung, Y.K.: Beams and plates on elastic foundations: A review. Prog. Struct. Eng Maths **7**, 174–182 (2005). https://doi.org/10.1002/pse.202
19. Psycharis, I.N.: Investigation of the dynamic response of rigid footings on tensionless Winkler foundation. Soil Dyn. Earthq. Eng. **28**, 577–591 (2008). https://doi.org/10.1016/j.soildyn.2007.07.010
20. Al-Shugaa, M.A.; Musa, A.E.S.; Al-Gahtani, H.J.: Analysis of corner supported plates under symmetrical loading. Arab. J. Sci. Eng. **44**, 8707–8715 (2019). https://doi.org/10.1007/s13369-019-03811-z
21. Celep, Z.; Turhan, D.; Al-Zaid, R.Z.: Circular elastic plates on elastic unilateral edge supports. J. Appl. Mech. **55**, 624–628 (1988). https://doi.org/10.1115/1.3125839
22. Celep, Z.: Circular plate on tensionless Winkler foundation. J. Eng. Mech. **114**, 1723–1739 (1988). https://doi.org/10.1061/(ASCE)0733-9399(1988)114:10(1723)
23. Celep, Z.; Turhan, D.; Al-Zaid, R.Z.: Contact between a circular plate and a tensionless edge support. Int. J. Mech. Sci. **30**, 733–741 (1988). https://doi.org/10.1016/0020-7403(88)90038-0
24. Celep, Z.; Turhan, D.: Axisymmetric vibrations of circular plates on tensionless elastic foundations. J. Appl. Mech. **57**, 677–681 (1990). https://doi.org/10.1115/1.2897076
25. Celep, Z.: Harmonic and seismic responses of a plate-column system on a tensionless Winkler foundation. J. Sound Vib. **155**, 47–53 (1992). https://doi.org/10.1016/0022-460X(92)90644-D
26. Güler, K.; Celep, Z.: Static and dynamic responses of a circular plate on a tensionless elastic foundation. J. Sound Vib. **183**, 185–195 (1995). https://doi.org/10.1006/jsvi.1995.0248
27. Celep, Z.; Gençoğlu, M.: Forced vibrations of a rigid circular plate on a tensionless Winkler edge support. J. Sound Vib. **263**, 945–953 (2003). https://doi.org/10.1016/S0022-460X(02)01472-4
28. Celep, Z.; Güler, K.: Static and dynamic responses of a rigid circular plate on a tensionless Winkler foundation. J. Sound Vib. **276**, 449–458 (2004)
29. Celep, Z.; Demir, F.: Circular rigid beam on a tensionless two-parameter elastic foundation. Z. Angew. Math. Mech. **85**, 431–439 (2005). https://doi.org/10.1002/zamm.200310183
30. Celep, Z.; Demir, F.: Symmetrically loaded beam on a two-parameter tensionless foundation. Struct. Eng. Mech. **27**, 555–574 (2007). https://doi.org/10.12989/SEM.2007.27.5.555
31. Celep, Z.; Güler, K.: Axisymmetric forced vibrations of an elastic free circular plate on a tensionless two parameter foundation. J. Sound Vib. **301**, 495–509 (2007). https://doi.org/10.1016/j.jsv.2006.09.029
32. Celep, Z.; Guler, K.; Demir, F.: Response of a completely free beam on a tensionless Pasternak foundation subjected to dynamic load,. Struct. Eng. Mech. **37**, 61–77 (2011). https://doi.org/10.12989/SEM.2011.37.1.061
33. Dimitrovová, Z.: Dynamic interaction and instability of two moving proximate masses on a beam on a Pasternak viscoelastic foundation. Appl. Math. Model. **100**, 192–217 (2021). https://doi.org/10.1016/j.apm.2021.07.022
34. Ghafarian, M.; Ariaei, A.: Forced vibration analysis of a Timoshenko beam featuring bending-torsion on Pasternak foundation. Appl. Math. Model. **66**, 472–485 (2019). https://doi.org/10.1016/j.apm.2018.09.029
35. Celep, Z.: Dynamic response of a circular beam on a Wieghardt-type elastic foundation. Z. Angew. Math. Mech. **64**, 279–286 (1984). https://doi.org/10.1002/zamm.19840640707
36. Celep, Z.: On the time-response of square plates on unilateral support. J. Sound Vib. **125**, 305–312 (1988). https://doi.org/10.1016/0022-460X(88)90285-4
37. Celep, Z.: Rectangular plates resting on tensionless elastic foundation. J. Eng. Mech. **114**, 2083–2092 (1988)
38. Celep, Z.; Güler, K.: Dynamic response of a column with foundation uplift. J. Sound Vib. **149**, 285–296 (1991). https://doi.org/10.1016/0022-460X(91)90637-Y
39. Guler, K.; Celep, Z.: Response of a rectangular plate-column system on a tensionless Winkler foundation subjected to static and dynamic loads. Struct. Eng. Mech. **21**, 699–712 (2005). https://doi.org/10.12989/SEM.2005.21.6.699
40. Celep, Z.; Gencoglu, M.: Forced vibrations of an elastic circular plate supported by unilateral edge lateral springs,. Struct. Eng. Mech. **83**, 451–463 (2022). https://doi.org/10.12989/SEM.2022.83.4.451
41. Dang, R.; Cui, Y.; Qu, J.; Yang, A.; Chen, Y.: Variable fractional modeling and vibration analysis of variable-thickness viscoelastic circular plate. Appl. Math. Model. **110**, 767–778 (2022). https://doi.org/10.1016/j.apm.2022.06.008
42. Celep, Z.; Özcan, Z.: Forced vibrations of an an elastic rectangular plate supported by a unilateral two-parameter foundation via the Chebyshev polynomials expansion. Struct. Eng. Mech. **90**, 551–568 (2024). https://doi.org/10.12989/SEM.2024.90.6.551
43. Celep, Z.; Özcan, Z.: Forced vibrations of an elastic triangular plate supported around its perimeter by a unilateral support via the Chebyshev polynomial expansion. Mech. Adv. Mater. Struct. **32**(15), 3608–3631 (2025). https://doi.org/10.1080/15376494.2024.2394986
44. Celep, Z.; Özcan, Z.; Güner, A.: Elastic triangular plate dynamics on unilateral Winkler foundation: analysis using Chebyshev polynomial expansion for forced vibrations. J. Mech. Sci. Technol. **39**(1), 65–79 (2025). https://doi.org/10.1007/s12206-024-1207-5
45. Celep, Z.; Özcan, Z.: Forced vibrations of an elastic rectangular plate supported by unilateral edge lateral springs. Arab. J. Sci. Eng. **48**(1), 13661–13678 (2023). https://doi.org/10.1007/s13369-023-07939-x
46. Huang, Y.; Zhao, Y.; Wang, T.; Tian, H.: A new Chebyshev spectral approach for vibration of in-plane functionally graded Mindlin plates with variable thickness. Appl. Math. Model. **74**, 21–42 (2019). https://doi.org/10.1016/j.apm.2019.04.012
47. Feng, W.J.; Yan, Z.; Lin, J.; Zhang, C.Z.: Bending analysis of magnetoelectroelastic nanoplates resting on Pasternak elastic foundation based on nonlocal theory. Appl. Math. Mech. **41**(12), 1769–1786 (2020). https://doi.org/10.1007/s10483-020-2679-7

48. Sadeghian, M.; Palevicius, A.; Janusas, G.: Nonlocal strain gradient model for the nonlinear static analysis of a circular/annular nanoplate. Micromachines **14**, 1052 (2023)
49. Gao, X.-L.; Zhang, G.Y.: A non-classical Mindlin plate model incorporating microstructure, surface energy and foundation effects. Proc. R. Soc. A Math. Phys. Eng. Sci. **472**, 20160275 (2016). https://doi.org/10.1098/rspa.2016.0275
50. Foyouzat, M.A.; Mofid, M.: An analytical solution for bending of axisymmetric circular/annular plates resting on a variable elastic foundation,. Eur. J. Mech. A. Solids **74**, 462–470 (2019). https://doi.org/10.1016/j.euromechsol.2019.01.006
51. SAP2000 Integrated Software for Structural Analysis and Design V20, 1988. Computers and Structures Inc, Berkeley, California.
52. Capurso, M.: A generalization of Wieghardt soil for two-dimensional foundation structures. Meccanica **2**, 49–54 (1967). https://doi.org/10.1007/BF02128154
53. Eringen, A.C.: Nonlocal Continuum Field Theories. Springer (2002)
54. Nami, M.R.; Janghorban, M.: Resonance behavior of FG rectangular micro/nano plate based on nonlocal elasticity theory and strain gradient theory with one gradient constant. Compos. Struct. **111**, 349–353 (2014). https://doi.org/10.1016/j.compstruct.2014.01.012
55. Papargyri-Beskou, S.; Beskos, D.E.: Static, stability and dynamic analysis of gradient elastic flexural Kirchhoff plates. Arch. Appl. Mech. **78**, 625–635 (2008). https://doi.org/10.1007/s00419-007-0166-5
56. Mason, J.C.; Handscomb, D.C.: Chebyshev Polynomials. Chapman & Hall, Boca Raton (2002)
57. Reddy, J.N.: Energy Principles and Variational Methods in Applied Mechanics. John Wiley (2002)
58. MATLAB and Statistics Toolbox Release 2012b, The MathWorks, Inc. 2012.
59. Leissa, A.W.: Vibration of Plates, NASA SP-160, 1969.
60. McLachlan, N.W.: Bessel Functions for Engineers. Clarendon Press, Oxford (1955)
61. Chopra, A.K.: Dynamics of Structures. Pearson, Harlow (2020)